Overview of the Stratigraphic and Structural Setting of Yucca Mountain, Nevada, USA

D. S. Sweetkind[1], **S. C. Beason**[2], and **D. C. Buesch**[3]

[1] U.S. Geological Survey, Denver Federal Center, MS 973, Denver, Colorado, 80225, U.S.A.
[2] U.S. Bureau of Reclamation, 1261 Town Center Dr., MS-475, Las Vegas, Nevada, 89117, U.S.A.
[3] U.S. Geological Survey, 1261 Town Center Dr., MS-475, Las Vegas, Nevada, 89117, U.S.A.

ABSTRACT

Yucca Mountain, Nevada, in the Basin and Range province of southwestern United States, consists of a thick Tertiary volcanic and sedimentary section that unconformably overlies a previously deformed Proterozoic to Paleozoic sedimentary section. Volcanic lithostratigraphic units are based on depositional, welding, crystallization, alteration, and fracture characteristics. Nine ignimbrites of formation rank and various interstratified tuffaceous deposits are the focus of most studies. The Tiva Canyon Tuff, which comprises most of the exposed rocks at Yucca Mountain, and the Topopah Spring Tuff, which contains the host rocks of a potential high-level radioactive-waste repository, are two of the most-studied formations. Although the Topopah Spring Tuff is typically 2 to 3 times thicker than the Tiva Canyon Tuff, in the central part of Yucca Mountain in the vicinity of the potential repository, these formations are similar in the proportional distribution and thickness of crystal-rich and crystal-poor members; occurrence of vitric, lithophysal, and nonlithophysal zones; and fracture characteristics of each unit.

The rocks at Yucca Mountain have been faulted, primarily during the Miocene, into east-dipping structural blocks that are bounded by north-striking, west-dipping normal faults. These block-bounding faults are typically spaced 1 to 4 km and have hundreds of meters of displacement. Within these structural blocks, strain is accommodated along intrablock faults, which are comparatively minor faults with a few tens of meters of displacement. The potential repository at Yucca Mountain is located within a relatively unextended block with few intrablock faults.

Fracture characteristics in the ignimbrites are primarily controlled by variations in degree of welding and crystallization. Nonwelded units have low fracture density but are cut by numerous small-offset faults, which represent these units' response to intrablock stress. Densely welded and crystallized units of the Tiva Canyon and Topopah Spring Tuffs have consistently higher fracture frequency and network connectivity than adjacent nonwelded and vitric units. Fracture intensity increases with degree of welding and crystallization within the densely welded deposits due to the presence of cooling fractures, and increased rock brittleness.

INTRODUCTION

Yucca Mountain, Nevada, has undergone intensive site characterization since 1982, as the Department of Energy examines the site for suitability as a potential long-term, high-level, nuclear waste repository. Yucca Mountain is approximately 160 km northwest of Las Vegas, Nevada, on the western edge of the Nevada Test Site (Fig. 1). The ability to license the site depends heavily on the area's natural attributes; subsequently the geology and hydrology of Yucca Mountain have been studied in extraordinary detail. Surface geologic mapping, an extensive program of boreholes, and a series of underground excavations have been undertaken to characterize the geology of the site. Surface investigations have included geologic mapping of the site at scales of 1:2,400 to 1:50,000, and fracture mapping of natural and cleared surface exposures. To help constrain geologic and hydrologic interpretations, 181 boreholes have been drilled and the cores, cuttings, borehole video recordings, and borehole geophysical logs collected from them have been examined and interpreted. Full-periphery geologic maps and fracture scanline surveys have been completed in the Exploratory Studies Facility (ESF), which is a 7.8-km long, 7.6-m diameter main tunnel, and the Cross Drift, a 2.7-km, 5-m diameter side tunnel (Fig. 2). The ESF consists of a North Ramp, a Main Drift, and a South Ramp. The Cross Drift originates in the North Ramp, traverses the potential repository block, and penetrates the Solitario Canyon fault on the west side of Yucca Mountain (Fig. 2). Geotechnical rock mass classification was performed in all underground excavations including ratings of rock quality designation (RQD), Q-system rating [1], and RMR rating [2, 3].

Much of the scientific investigation has focused on a relatively undeformed, fault-bounded structural block that would be the primary host area of the potential repository. This potential repository block has been termed the central block [4] (Fig. 2). For the purposes of this paper, the central block of Yucca Mountain is bounded on the east and north by the Bow Ridge fault and Drill Hole Wash fault, and on the south and west by the Solitario Canyon fault, and Abandoned Wash, respectively [4]. Within the central block, the potential repository block is presently bounded on the west by the Solitario Canyon fault, and on the east by the Ghost Dance fault (Fig. 2). If the potential repository footprint is expanded, the repository might extend beyond either of these structural features.

GEOLOGIC SETTING

The Yucca Mountain area lies along the southwest margin of the Basin and Range province in a stratigraphically diverse and structurally complex region in which a thick Tertiary volcanic and sedimentary section unconformably overlies previously deformed Proterozoic through Paleozoic rocks. These rocks were deformed by complex Neogene extensional and strike-slip faults superimposed on late Paleozoic to mid-Mesozoic folds and thrusts [5, 6]. Yucca Mountain is within the northwest-trending Walker Lane belt, which records transtensional deformation, manifested on a regional scale by right-oblique slip along northwest-striking faults, and left-oblique slip along northeast-striking faults [7].

Yucca Mountain and Crater Flat to the west (Fig. 1) lie within a 25-km-wide internally faulted half-graben [8, 9] that is bounded on the west side by the Bare Mountain fault, a major east-side-down fault [10, 11, 12]. Miocene volcanic rocks within this half-graben are preserved in several predominantly east-dipping blocks that are bounded by north- to northeast-striking, west-dipping normal faults.

The Miocene volcanic rocks at Yucca Mountain form part of the southwestern Nevada volcanic field (SWNVF), which was active from 7.5 to 15.1 million years, contains seven identified calderas and as many as seven additional, inferred calderas [13]. The SWNVF deposits consist of regionally extensive and large-volume ignimbrites, numerous less extensive and smaller volume ignimbrites, many lava flows and lava domes, fallout tephra deposits, and minor redeposited tuffaceous and epiclastic rocks [13, 14, 15, 16, 17, 18].

Stratigraphic and structural setting, Yucca Mountain

Based on seismic reflection and gravity data, the Tertiary section is interpreted to be up to 3.5 km thick in western Crater Flat [10], but thins eastward to between about 1.5 and 2.5 km in the vicinity of Yucca Mountain. Several boreholes at Yucca Mountain are between 1500 and 1900 m deep [19], yet bottom in Tertiary strata. Tertiary rocks are 1,244-m thick in borehole UE-25p#1 [20], which is located about 2 km east of Yucca Mountain and is the only borehole to penetrate the entire section. It is not clear however, whether the Tertiary-Paleozoic contact within UE-25p#1 is an unconformity or fault contact and this hole has been interpreted to be drilled on a Paleozoic high [19].

The volcanic sequence at Yucca Mountain includes, in descending order, rocks belonging to the Timber Mountain Group, the Paintbrush Group, the Calico Hills Formation, the Crater Flat Group, and a number of older tuffs [13] (Fig. 3). Most of the exposures in the vicinity of the central block of Yucca Mountain are tuffs within the Paintbrush Group (Fig. 3) [4, 13, 21, 22]. Volumetrically, the most significant formations within the Paintbrush Group are the Tiva Canyon and Topopah Spring tuffs; two densely welded and crystallized ignimbrites that are separated by a comparatively thin interval of mostly nonwelded, vitric pyroclastic deposits. The Tiva Canyon Tuff is the most extensively exposed unit at the surface of Yucca Mountain, and the Topopah Spring Tuff includes rocks in which the potential repository would be located; therefore, these two formations and their detailed lithostratigraphy form the fundamental framework of many studies.

HYDROLOGIC SETTING

The hydrologic setting of Yucca Mountain reflects the arid climate and geologic history of the northern Mojave Desert. Yucca Mountain receives only an average of 166 mm of annual precipitation [23] that occurs as localized summer thunderstorms and more broadly distributed winter rain or snow. The hydrogeologic system near the central block of Yucca Mountain consists of a 500- to 750-m-thick unsaturated zone overlying a relatively flat regional water table [24]. The potential repository would be excavated roughly midway in the unsaturated zone within the crystallized and densely welded Topopah Spring Tuff, about 250 m above the water table and 250 to 375 m below the surface.

The water table beneath the central portion of Yucca Mountain generally lies within the volcanic rocks of the Calico Hills Formation or the Crater Flat Group [25]. To the west of Yucca Mountain there is a moderate (30 m of relief) hydrologic gradient, and to the north is a possible steep (300 m relief) gradient [26]. This northern steep gradient has been variously interpreted as resulting from structures in the pre-Calico Hills Formation rocks [27], or as a perched or semi-perched water system [28, 29].

Much of the Yucca Mountain site characterization effort has been geared toward understanding how water percolates through the mountain and how such migration affects the mountain's ability to isolate radionuclides from the accessible environment. Most of the crystallized and densely-welded tuffs have very low matrix permeabilities [30]; consequently, fracture networks and faults are the primary pathways for gas and water flow into and out of the potential repository. Fracture-dominated flow in the welded portions of the Tiva Canyon and Topopah Spring Tuffs changes to matrix-dominated flow in the high-permeability comparatively unfractured units between the Tiva and Topopah, and in the generally nonwelded Calico Hills Formation underlying the Topopah Spring Tuff [24].

LITHOSTRATIGAPHY

Volcanic rocks have been, and continue to be, a major focus of stratigraphic studies being conducted as part of the site characterization program at Yucca Mountain. Basic data on the thickness, lateral extent, stratigraphic relations, and lithologic characteristics of the rocks in both surface and subsurface settings have been obtained through studies of boreholes and cores from these boreholes [e.g., 20, 31, 32, 33, 34, 35, 36, 37, 38], as well as from geologic mapping at the surface [21] and in the underground excavations. These lithostratigraphic studies have resulted in the following advances: 1) the identification of lithostratigraphic units based on compositional, depositional, welding, crystallization, alteration, and fracture characteristics; and 2) the use of rock properties, including density and porosity, in the identification of lithostratigraphic units, and related hydrogeologic and thermal-mechanical units.

The Tiva Canyon and Topopah Spring Tuffs both have an upper crystal-rich (> 10 percent phenocrysts) quartz latite member and a more voluminous lower crystal-poor (< 5 percent phenocrysts) rhyolitic member [18, 39] with a relatively thin transition in phenocryst abundance and chemical composition between members. Locally, each has minor accumulations of pumice and lithic clasts. At Yucca Mountain, these formations appear to have been deposited by progressive accumulation of pyroclastic-flow deposits associated with climactic eruptions. Zones, subzones, and intervals are identified on the basis of textures, structures, lithic fragments, bedding (all products of depositional processes), zones of welding and crystallization (related to post-depositional processes), and geometry and surface roughness of fractures (related to mechanical properties of the rock) [39]. Within the Paintbrush Group, the Topopah Spring Tuff is commonly 2 to 3 times thicker than the Tiva Canyon Tuff (350 m versus 150 m, respectively), yet in the central Yucca Mountain area these formations are strikingly similar in relative distribution and thickness of the crystal-rich and crystal-poor members, occurrence of vitric, lithophysal, and nonlithophysal zones, and fracture characteristics of each unit [39]. However, away from the central block in northern and southern Yucca Mountain and in Crater Flat, similarity between these tuffs decreases as a result of lateral facies changes. Within the central block at Yucca Mountain, the overlap of depositional and zonal features typically results in an internal stratigraphy that is generally stratiform [36, 39, 40, 41]. Formations, bedded tuff and in some cases, zones in the Tiva Canyon and Topopah Spring Tuffs, can be traced across much of the area depicted in Figure 2 [21, 22]. Due to the need for precise stratigraphic location in support of various sampling and testing programs in boreholes and the underground excavations, a detailed stratigraphic nomenclature has been devised for rocks of the Paintbrush Group [39, 40, 41] and the Crater Flat Group [36, 42] (Fig. 3). In this scheme, the first three letters of the stratigraphic symbol denote the formal formation name (such as Tpt for the Topopah Spring Tuff) [13](Sawyer and others, 1994D). The fourth letter denotes the member, "r" for crystal-rich and "p" for crystal-poor; letters that follow denote the zonal designation, such as "ll" for lower lithophysal zone".

Between the Tiva Canyon and Topopah Spring Tuffs is an interval of nonwelded vitric pyroclastic fall, bedded tuffs and reworked material [40]. At the north end of Yucca Mountain, extending to the northern part of the central block, this interval also contains two voluminous pyroclastic flows, the Yucca Mountain and Pah Canyon Tuffs (Fig. 3), and several other small volume pyroclastic flows and lava flows. These units were lumped with the welding transitions of the overlying Tiva and underlying Topopah as the Paintbrush Tuff nonwelded hydrogeologic unit [30].

Underlying the Topopah Spring Tuff, the Calico Hills Formation consists of lava flows and interbedded tuffs at the north end of Yucca Mountain, and interbedded ignimbrites and fallout tephra to the south [36]. In the central block, the formation changes from being pervasively vitric in the southwest to pervasively zeolite-altered in the northeast [36]. The underlying rocks of the Crater Flat Group, the Prow Pass, Bullfrog, and Tram Tuffs, each consist of several ignimbrites and fallout tephra deposits that have been welded and crystallized, and where vitric, altered to zeolite and clay minerals [36]. The Prow Pass, Bullfrog, and Tram Tuffs are differentiated from each other based on variations in phenocrysts, pumice, lithic clasts, and interstratified bedded tuffs [36, 42].

Lithostratigraphic Units and Rock Properties

During site characterization at Yucca Mountain, three primary stratigraphic systems were developed to investigate the distribution of lithostratigraphic, hydrogeologic, and thermal-mechanical units, and each system developed its own nomenclature (Fig. 3) [21, 30, 36, 39, 43, 44, 45]. Common to all these systems are the properties of bulk rock density and porosity, and therefore the systems are only semi-independent with lithostratigraphy often serving as the common framework. Where there are changes in these rock properties, it is reasonably expected that there are commensurate changes in many of the associated hydrogeologic and thermal-mechanical properties. Thus, it has been suggested that lithostratigraphic, hydrogeologic, and thermal-mechanical units share some common boundaries [39, 40]. Many of the boundaries differ in stratigraphic position, because of differences in the definitions of time-stratigraphic boundaries relative to hydrologic and thermal-mechanical boundaries.

Hydrogeologic Properties

Hydrogeologic properties are used to divide the unsaturated zone at Yucca Mountain into five major bedrock hydrogeologic units: Tiva Canyon welded (TCw), Paintbrush nonwelded

(PTn), Topopah Spring welded (TSw), Calico Hills nonwelded (CHn), and Crater Flat (CFu) [30] (Fig. 3). These five major units have been divided into 30 smaller hydrogeologic units [44] that were used as the stratigraphic framework in a hydrogeologic model of the unsaturated zone of Yucca Mountain [46]. Most hydrogeologic boundaries are between 0.5 m and a few meters of lithostratigraphic contacts [41]. Porosity measured on core, and the calculated "differential porosity", correlate well with lithostratigraphic units in the vitric, zeolitic, and crystallized rocks, and this correlation is exemplified in borehole UZ#16 (Fig. 4). Based on the hydrogeologic properties of vitric rocks from the welding transitions in the Topopah Spring Tuff (units tpv1, 2 & 3 and trv 1, 2 & 3, Fig. 4), rocks from the moderately welded zone contain the most important and significant variations in properties; therefore, identification of this zone has been important for understanding and modeling the hydrogeologic data and model parameters. Depositional textures, including grain-size and sorting in fallout tephra and ignimbrites, can form localized discontinuities in porosity and permeability. The amount and type of alteration can also create flow paths for water, as exemplified by the water seeps in UZ#16 (Fig. 4).

Geophysical Properties

A typical suite of borehole geophysical logs at Yucca Mountain includes caliper, density, induction, resistivity, neutron, and gamma-ray logs, and for a few boreholes there are magnetic, p- and s-velocity logs, and borehole gravimeter logs [47]. Porosity and saturation values are calculated from the density, induction, resistivity, and neutron logs [48]. Many lithostratigraphic features, including contacts, produce changes in geophysical properties. Some previously described features do not have well-developed geophysical log signatures, and other features that were not initially emphasized actually correlate closely with geophysical data [49]. Welding, crystallization, and alteration are important geologic controls on geophysical log response, and locally the grain size, sorting, and lithic clast content can also affect log response [47, 49, 50]. Detailed correlations of lithostratigraphic features and geophysical data can be made for units less than 1-m thick. Where gradational changes in rock property values are several meters thick, values such as density can facilitate consistent identification of contacts [49].

Thermal-mechanical Properties

Thermal-mechanical stratigraphic units have been identified in the volcanic rock sequence at Yucca Mountain from the Tiva Canyon Tuff to the upper part of the Tram Tuff [45] (Fig. 3). These units were defined for design and performance analyses and were based on rock properties, rather than classic geologic criteria. However, most of the thermal-mechanical unit boundaries in the Paintbrush Group approximate lithostratigraphic contacts. In the Crater Flat Group, the thermal-mechanical unit boundaries are closely associated with lithostratigraphic facies [42]. Figure 6 illustrates the variations in porosity, density, p- and s-wave velocity, Young's modulus, and ultimate strength plotted versus depth within the Topopah Spring Tuff and the lower part of the Tiva Canton Tuff for borehole NRG-6. A typical distribution of thermal-mechanical property data in borehole NRG-6 (Fig. 6) illustrates that the thermal-mechanical data can be used to determine general properties of the units, but typically it is difficult to identify a unique contact between units.

Lithostratigraphic Units and Geologic Processes

Welding

Welding in pyroclastic rocks results in the viscous deformation of glass shards and pumice clasts and a decrease in porosity. At Yucca Mountain there are four zones of welding: nonwelded, partially, moderately, and densely welded [39]. Fallout tephra and thin ignimbrite beds are typically nonwelded, but thick ignimbrites can be welded to varying degrees. The zones are vertically distributed in a simple welding unit with nonwelded rocks at the top and bottom and increased welding toward the center of the deposit [51]. In the vicinity of the central block of Yucca Mountain, the Tiva Canyon, Yucca Mountain, Pah Canyon and Topopah Spring Tuffs form simple welding units [40], despite the great thickness and some variation in depositional features such as size and abundance of phenocrysts, pumice, and lithic clasts [39]. Both the Tiva Canyon and Topopah Spring Tuff are characterized by a thick, densely welded, crystallized center portion and welding transitions at the upper and lower margins of the flow. The Prow Pass, Bullfrog, and Tram Tuffs form compound welding units [36, 42].

The degree of welding can be determined through measurements of bulk density and porosity. Based on correlations of detailed lithostratigraphic descriptions to measured density, and porosity [39, 44, 53], variably welded, vitric, tuff at Yucca Mountain may be classified as follows: vitric nonwelded rocks have densities less than 1.29 g/cm^3 and porosities of 45 percent or greater; partially welded vitric rocks have densities between 1.29 and 1.75 g/cm^3 and porosities between 25 and 45 percent; moderately welded vitric rocks have densities between 1.75 and 2.12 g/cm^3 and porosities between 10 and 25 percent; and densely welded vitric rocks have densities greater than 2.12 g/cm^3 and porosities of less than 10 percent. Crystallized rocks have similar ranges in density and porosity for the four zones of welding, but typically have slightly (about 2 to 5 percent) greater porosity and concomitantly lower density ranges compared to vitric rocks. Densely welded and crystallized rocks containing lithophysae can have bulk porosity (based on calculated porosity from geophysical logs) of as much as 40 percent, although the porosity of the groundmass (measured on core) can be similar to the porosity of nonlithophysal rocks. Rocks in which vapor-phase corrosion and mineralization occurred can have density and porosity values that differ significantly from the ranges for vitric and crystalline rocks [41]. Data from borehole UZ#16 displays many of these relations of porosity in lithostratigraphic units from the Tiva Canyon Tuff to the Prow Pass Tuff (Fig. 4).

Crystallization

General characteristics of crystallization in nonwelded to densely welded ignimbrite deposits have been described by Smith [51, 52, 54]. Crystallization of the welded ignimbrites at Yucca Mountain occurred at high temperature (greater than several hundreds of degrees celsius) of the vitric rock mass to form the groundmass, and directly from a vapor phase. In the high-temperature, crystallized Tiva Canyon and Topopah Spring Tuff, quantitative mineralogical data indicate the abundance of feldspar as 55 to 70 percent, quartz as 0 to 20 percent, cristobalite as 5 to 30 percent, tridymite as 0 to 25 percent, and other minerals 0 to 2 percent [55]. Quantitative mineralogical data from borehole UZ#16 demonstrates the type of variations in data that occur in the crystallized rocks of the Tiva Canyon, Topopah Spring, and Prow Pass Tuffs (Fig. 4). Many crystallization textures and associated colors of the groundmass appear to relate to crystallization in the presence or absence of vapor [56, 57].

Vapor-phase Processes

As the process of welding decreases porosity, there must be a concomitant redistribution of the initially interstitial vapor by three main processes: 1) entrapment of vapor along grain boundaries in the most densely welded parts of the deposits, 2) intergranular porous matrix flow, and 3) flow along fractures [56]. Vapor-phase activity accompanies the welding and crystallization of the tuffs and results in corrosion of volcanic glass and the deposition of high-temperature minerals from the vapor-phase [41, 57]. Textural evidence for the corrosion of glass includes cavernous pumice clasts where the internal walls have been removed by corrosion, and well-preserved shard outlines where the shards themselves have been replaced by void space. Corrosion occurs in nonwelded to densely welded rocks, and is well developed in the upper parts the Tiva Canyon, Topopah Spring, and Prow Pass Tuffs. Corrosion is often most strongly manifested in moderately welded rocks near the contact between vitric and crystalline rocks, but can be widely distributed throughout the tuff as well [39, 41]. Corrosion results in secondary porosity that can be much greater than exists in non-corroded tuffs with similar degrees of welding [39, 40, 41].

Vapor-phase minerals typically contain abundant euhedral crystals of tridymite, smaller amounts of sanidine, and very small amounts of other minerals such as specular hematite and manganiferous biotite and amphibole [39, 58]. Vapor-phase crystals grow in primary pore spaces in nonwelded to moderately welded tuffs, and in densely welded rocks in secondary pore spaces such as lithophysal cavities or casts of glass shards corroded by vapor, and along fractures [39].

Lithophysae and other vapor-phase features

Vapor-phase features observed in the Tiva Canyon and Topopah Spring Tuffs include lithophysae, vapor-phase spots, vapor-phase streaks, stringers and partings. Lithophysae are bubble-like cavities surrounded by finely crystalline minerals and they occur where vapor concentrates in the densely welded part of ignimbrites [54]. Within the central block at Yucca Mountain, lithophysae occur in the Tiva Canyon and Topopah Spring Tuffs where they form the crystal-rich lithophysal (Tpcrl and Tptrl, respectively, Fig. 3) and crystal-poor upper and lower lithophysal zones (in the Tiva Canyon Tuff, Tpcpul and Tpcpll, respectively; in the Topopah Spring Tuff, Tptpul and Tptpll, respectively, Fig. 3). Locally they occur in minor amounts in nonlithophysal zones [39]. At the north end of Yucca Mountain, lithophysae also occur within the Yucca Mountain and Pah Canyon Tuffs. Lithophysae consist of several parts including a 1-cm to 1-m sized cavity, vapor-phase mineral coating on the cavity wall, a 2-mm- to 3-cm-wide light gray to light pink rim, and a 1- to 3-mm-wide reddish purple border that differs from the adjacent groundmass color [39] (Fig. 5). Lithophysae form as part of the welding process of ductile and viscous glass, and occur prior to crystallization that results in a rigid rock mass [54]. Lithophysae formed where the vapor accumulated and attained super-lithostatic pressure, thereby inflating and deforming the vitric rock mass [56]. Lithophysae vary in shape from simple spheres to lens to irregular cavities formed by multiple coalesced lithophysae to breached and partially deflated cavities that merge with vapor-phase mineralized fractures [57]. Many lithophysae merge with or are intersected by veinlets or vapor-phase mineral-coated fractures that probably were pathways for vapor to enter or exit the lithophysal cavities. However, many features, such as vapor-phase streaks, veinlets, stringers have no apparent connection to fractures with visible aperture and probably indicate crystallization of glass in the presence of a vapor-phase [56].

Vapor-phase spots are typically associated with lithophysae; spots are similar to lithophysae, except they have no central cavity [39]. Some spots might be part of a lithophysal rim, but some contain a core consisting of a phenocryst or lithic fragment, or a small isolated piece of the groundmass. The shape of lithophysae and spots and the width of rims on lithophysae can be characteristic of individual zones or subzones [19, 32, 39, 56].

Most contacts of lithophysal and nonlithophysal units typically have a concentration of streaks, veinlets, stringers, and partings and moderately dipping fractures (Fig. 5 a,b,c). Many vapor-phase partings consist of anastomosing partings or a multitude of short discontinuous veinlets that can be traced as a discrete parting for many tens of meters (Fig. 5d). The combination of these features forms the transition between the units and results in a network of vapor-phase mineral-coated fractures [56].

Alteration

Alteration of the volcanic rocks at Yucca Mountain may be subdivided into three general classes: 1) vapor-phase alteration (discussed above) that accompanies the crystallization and welding of the host tuff, occurs at high temperatures and is caused by the redistribution of interstitial magmatic vapor products; 2) moderate-temperature alteration, which is typically clay-silica alteration that occurred at temperatures between 100 and 200 °C, and appears to be the result of local hydrothermal cells produced by the interactions between downward-percolating meteoric waters with the still-cooling tuff; and 3) diagenetic alteration, typically zeolitic or argillic, that occurs at near-ambient-temperatures and is the result of the interaction of tuff with percolating waters or with groundwater.

Moderate-temperature alteration results in locally spectacular, but spatially limited, zones of smectite-zeolite or feldspar-cristobalite assemblages. This alteration has been noted in several places around Yucca Mountain at or near devitrified-vitric transitions. Examples of this type of alteration include local argillic alteration near the top of the Topopah Spring Tuff and in the overlying bedded tuff (Tpbt2, Fig. 3) both at the surface [40] and in the North Ramp of the ESF [59]. This alteration is interpreted to be the result of local hydrothermal alteration of reactive volcanic glass at the vitric-crystallized transition zone during the late-stage cooling of thick tuff deposits [40, 59, 60].

The most extensive post-cooling mineralogic change affecting the rocks at Yucca Mountain has been the zeolitization of nonwelded vitric tuffs. In the affected rocks, the vitric component has been altered to the zeolite clinoptilolite with or without lesser amounts of mordenite, smectite, heulandite, opal, and cristobalite, and other minor phases [55]. Most zeolitized tuffs are products of diagenetic alteration in which the original glass dissolved and the zeolites precipitated at ambient temperatures in a water-rich environment [61]. Pervasively zeolitic rocks occur throughout much of the lower parts of the Topopah Spring Tuff, Calico Hills Formation, and in the Prow Pass, Bullfrog, and Tram Tuffs [62]. Because zeolitic alteration preferentially affects vitric material, the original distribution pattern of devitrified and vitric tuffs largely determined the locations of zeolitic and nonzeolitic rocks in those parts of Yucca Mountain where the rocks have been subject to zeolitization. The distribution of diagenetically altered zeolitic rocks is of particular importance for nuclear waste repository performance, as the transition marks changes in the hydraulic and sorptive properties of nonwelded tuffs [63].

STRUCTURE

Fault Types at Yucca Mountain

Yucca Mountain consists of a series of gently east-dipping blocks of volcanic strata bounded by normal faults. The block-bounding faults are north-striking, west-dipping faults spaced one to four km apart [64, 22]. Field mapping of the Miocene Paintbrush Group tuffs shows that these faults have commonly experienced hundreds of meters of Tertiary normal-sense displacement with a subordinate component of strike-slip motion [4, 21, 22, 65]. Trenches have been constructed across all of the major faults in the vicinity of the potential repository to document paleoseismic activity; in some cases, Quaternary offset has been documented on the block-bounding faults [66, 67]. In the site area (Fig. 2), block-bounding faults include (from west to east) the Windy Wash, Fatigue Wash, Solitario Canyon, Dune Wash, Bow Ridge, Midway Valley, and Paintbrush Canyon faults. Fault scarps commonly dip 50°-80° to the west, with scattered dips in the 40°-50° and 80°-90° ranges. Block-bounding faults are commonly linked by relay structures [22], complex zones of faulting that intersect block-bounding faults at oblique angles and transfer displacement between block-bounding faults.

In addition to the overall influence of the major block-bounding faults, structural style at Yucca Mountain varies from north to south as a result of southwestward-increasing extension and vertical-axis rotation [9, 64, 68]. North of the central part of Yucca Mountain is a little-extended terrane characterized by strike-slip faults that connect the Solitario and Bow Ridge faults. South of the central block is a dramatic increase in the magnitude of extension accompanied by significantly different structural styles [21, 22]. Block-bounding faults in northern Yucca Mountain are typically simple, north-striking, steeply dipping (70 to 80 degrees) faults, whereas these faults in the more-extended southern part of the mountain have northeasterly strikes, moderate fault-plane dips (55 to 75 degrees), greater fault zone width and complexity, and a significant component of left-lateral slip [22, 64]. In areas within the blocks, the transition is expressed by the appearance of numerous closely spaced minor faults that coalesce and gain displacement to the south.

Most offset on faults in the Yucca Mountain vicinity occurred during or subsequent to the major pyroclastic eruptions of the Paintbrush and Timber Mountain Groups between 11.4 and 12.7 Ma [22, 64]. Fault-slip analyses support a mid-Miocene age as the main period of motion of Yucca Mountain faults. The north-striking fault pattern at Yucca Mountain is consistent with Miocene regional strain patterns, with an overprint of caldera-related deformation in northernmost Yucca Mountain [69]. Fault activity persisted through at least middle to late Quaternary time on many block-bounding faults, although the cumulative displacement and rates of activity diminished significantly during the Quaternary [65].

Intrablock faults lie entirely within the structural blocks defined by the block-bounding faults [4, 22]. In the central block, intrablock faults are nearly vertical, have 1-30 m of displacement, and typical mapped lengths of less than 1 km [4]. Intrablock faults, such as the Ghost Dance, Abandoned Wash, and Busted Butte faults are marked by zones that widen upward near the surface, becoming frameworks of upward-splaying faults [4]. In many cases, intrablock faults appear to represent local structural adjustments in response to displacements on the block-bounding faults. In a few cases, intrablock faults are expressions of hanging-wall or footwall deformation that affects the block within a few hundred meters of the block-bounding faults. For example, a number of small faults were intersected in the North Ramp of the ESF to the west of the Bow Ridge fault.

In the vicinity of the central block, many small faults (those with trace lengths of about 200 m or less and 1 to 10 m of displacement) are vertically and laterally discontinuous [21, 70]. In surface exposures, many of these minor intrablock faults are parallel to the dominant orientations of cooling fractures in the Tiva Canyon Tuff, of which the two most prominent sets have orthogonal northeasterly and northwesterly strikes [71]. In subsurface exposures of the Topopah Spring Tuff, long, smooth fractures that are probable cooling joints often display small amounts (less than 1 m) of offset. In both surface and subsurface exposures, thin (1 cm thickness) tabular tectonic breccia bodies are observed along fractures interpreted to be cooling joints. These observations suggest that cooling joints served as planes of preexisting weakness that were reactivated as small faults during extension. Offset along individual discontinuous faults strands appears to be accommodated by strain transfer across overlapping fault tips or manifested as distributed brecciation in regions between faults [70, 72, 73].

Block-Bounding Faults in the Vicinity of the Potential Repository

Deformation associated with the block-bounding faults at Yucca Mountain affects several major repository issues such as the volume and quality of rock available for underground construction of the potential repository, the delineation of fast hydrologic flow paths, and seismic hazard assessments. The central block of Yucca Mountain that includes the potential repository is bounded by the Bow Ridge and the Solitario Canyon faults; the ESF crosses the north end of the Dune Wash block-bounding fault [4].

Bow Ridge fault

The Bow Ridge fault forms the eastern boundary of the central block and is well exposed in trenches just west of Exile Hill, where it has been studied extensively [67]. In the North Ramp of the ESF, the Bow Ridge fault was encountered approximately 200 m from the tunnel portal. The fault as exposed in the tunnel is north-striking, and dips 75° W, with approximately 128 m of primarily dip-slip, down-to-the-west offset. This amount of offset matches well with preconstruction estimates of 125 m derived from borehole data [74]. The rubble zone along the fault is approximately 2.7 m thick, and composed of three uncemented breccia zones. The breccias contain clasts derived primarily from nonwelded rocks in the hanging wall of the fault zone (pre-Rainier Mesa Tuffs), with minor amounts of welded clasts derived from the footwall (Tiva Canyon Tuff, lower lithophysal zone). A striking feature of the fault exposure at this location is the lack of footwall deformation. Only 0.5 m into the footwall, the rock is relatively unfractured. The absence of footwall deformation is common in northern and central Yucca Mountain, and is a feature of both block-bounding and intrablock faults across the site. West of the Bow Ridge fault are north- and northwest-striking faults, which have normal displacement both down-to-the-west and down-to-the east. These faults are the result of hanging-wall deformation associated with the Bow Ridge fault [4].

Solitario Canyon fault

The Solitario Canyon fault forms the western boundary of the central structural block and is the longest continuously exposed fault at Yucca Mountain [65](Fig. 9e). West-side down displacement varies considerably along strike from a few tens of meters at the head of Solitario Canyon to more than 500 m at its southern end [21, 22]. In the vicinity of the Cross Drift, the fault zone is composed of two major strands – a western, older strand [65] striking north-northeast with approximately 70 m of offset [75], and a larger, more recently active eastern strand with approximately 230 m of offset. These two faults bound a zone characterized by numerous fault splays and local intense brecciation that includes panels of tectonically intermingled Tiva Canyon and Topopah Spring Tuffs in the fault zone [4, 22]. Areas of abundant fault splays appear to be associated with fault bends or, locally, where displacement along the Solitario Canyon fault zone is being transferred from the eastern to the western fault strand.

The eastern strand of the Solitario Canyon fault is exposed in the Cross Drift where it strikes north and dips 63° to the west. Dip-slip offset along the fault as exposed in the tunnel is approximately 230 m, but slickensides on the fault plane indicate there also may be a strong oblique-slip component. The total thickness of the disturbed zone adjacent to the fault (both footwall and hanging wall) at this locale is nearly 70 m. At the tunnel level, the footwall is composed of a matrix-supported breccia formed of clasts of rock from the lower nonlithophysal zone of the Topopah Spring Tuff. The hanging wall is composed of upper lithophysal zone of the Topopah Spring Tuff – a stratigraphic separation of approximately 227 m. In the zone between the hanging and footwalls is a breccia zone formed exclusively of clasts from the crystallized, moderately welded, and vitric, nonwelded to moderately welded rocks of the crystal-poor Tiva Canyon Tuff. This section of stratigraphically higher rocks suggests that the fault plane dilated substantially at some time during post-Tiva movement, allowing rocks from above to drop into the Topopah-bounded fault zone. There is no evidence of weathering, or other indication that the dilated opening was exposed for any length of time, so this breccia may represent a very short-term event in terms of how long the fault plane was open. The fault zone exhibits very little non-mechanical alteration along the fault plane, or in the adjacent rock. The footwall of the fault zone in the lower nonlithophysal zone of the crystal-poor Topopah Spring Tuff displays some hematitic staining, presumably from meteoric water.

Dune Wash fault

The South Ramp of the ESF intersects the northern end of the Dune Wash fault approximately 1090 m from the South Portal. Offset on the Dune Wash fault at the surface is about 50 m at this latitude, although offset rapidly increases to the south [22]. In surface exposures, the fault consists of a pair of left-stepping faults that appear to have both west-side-down and left-lateral motion. Left steps in the fault zone create local dilatant zones where rock units stratigraphically between hanging wall and footwall lithologies are preserved. The Dune Wash fault as exposed along the South Ramp is composed of a pair of northwest-striking fault planes. In tunnel exposures, the faults have a combined down-to-the-west normal offset of approximately 52 m. The individual fault planes are composed of clast-supported breccias 0.25 to 0.5 m thick. Between the two planes is a series of steeply tilted, sheared rocks of various lithologies that represent intermediate amounts of offset.

Intrablock Faults in the Vicinity of the Potential Repository

Intrablock faults in the vicinity of the potential repository central block include the largest intrablock fault, the Ghost Dance fault [4, 21], which has up to 25 m of stratigraphic offset. Other faults include the Sundance fault and faults in the hanging-wall of the Bow Ridge fault (part of the "imbricate fault zone" of Scott [64] and the Drill Hole Wash fault (Fig. 2).

Ghost Dance fault

The Ghost Dance fault (Fig. 2) is a 7-km-long, north-striking, normal fault, steeply west-dipping (75°-85°) with down-to-the-west displacement. The displacement, amount of brecciation, and number of associated splays vary considerably along its trace [76]. In surface exposures, the northern third of the fault is a relatively narrow zone of breccia (2 to 4 m wide) with as much as 6 m of down-to-the-west displacement. Down-to-the-west displacement increases southward reaching a maximum of 27 m along the central portion of the Ghost Dance fault zone, and fracturing extends for tens of meters into the hanging wall of the principal splay of the fault [77]. Underground, two alcoves were excavated from the ESF specifically to intercept the Ghost Dance fault near the area of greatest offset. In Alcove 7, the fault is north-striking, dipping approximately 72° W, with approximately 25 m, of down-to-the-west offset. In Alcove 6, approximately 1200 m north of Alcove 7, the fault has only 3-5 m of offset and it has only 0.1 m of offset in the Cross Drift, 1000 m north of Alcove 6. Three hundred meters north of the Cross Drift, the Ghost Dance fault is not found in the ESF North Ramp. In the alcoves, thoroughly brecciated rock along the fault plane is 0.6 to 1.0 m thick, with no apparent increase in fracture intensity near the fault in the footwall, but approximately 4 m of intensely fractured rock in the hanging wall. In the Cross Drift, breccias along the fault are only 0.02-0.1 m thick, with approximately 0.4-0.6 m of intensely fractured rock bordering the zone. Although Day and others [4] observed vertical upward splaying of the Ghost Dance fault, at the depth of the ESF excavation - approximately 200 m - the faults splays have generally coalesced into a single zone. Offset decreases abruptly along the southern third of the fault where the fault splits into several minor splays. To the south, a western splay of the Ghost Dance fault has only 1.2 m of offset where encountered by the Main Drift of the ESF, about 700 m south of Alcove 7. At this location, the fault zone consists of only 0.25 m of clast-supported breccia, with minor fractured zones surrounding the breccia on both foot- and hanging walls.

Sundance fault

The Sundance fault [70, 78] in surface exposures has a northwesterly strike (N 20° W. - N 30° W.) and dips 80°-90° to the northeast. The maximum width of the Sundance fault zone is about 75 meters and the cumulative northeast-side-down vertical displacement across the fault zone does not exceed 11 m [70]. Individual fault strands in the Sundance fault zone are laterally and vertically discontinuous. The fault zone is interpreted to have exploited pre-existing cooling fractures, so that the width of the zone and the number of splays were controlled by the fracturing characteristics of each stratigraphic interval [70]. The Sundance fault exposed in the ESF Main Drift underlies the southeast distal end of the Sundance fault zone as mapped at the surface [70]. In the ESF, the fault is a northwest-striking feature with well-developed, subhorizontal slickenlines with an indeterminate amount of displacement. Kinematic indicators along the fault plane indicate right-lateral offset, but distinct markers are not present. In the ESF, the Sundance fault and associated structures dip steeply to the west, which contrasts with the vertical to steep easterly dips at the surface. Individual fault strands are discontinuous and appear to have small displacement in this part of the Sundance fault zone, both in the ESF and at the surface.

Drill Hole Wash fault

The Drill Hole Wash fault consists of a principal strand along the northeast edge of Drill Hole Wash. The northeastern trace of the fault was intersected in a borehole in the wash [79], and probable related faults are mapped at the surface adjacent to the wash [4]. The Drill Hole Wash fault was long thought to be a major, northwest-striking feature until exposed by underground excavation. Boreholes and surface-based geophysics indicated that the feature was tens of meters thick and, because of the large valley developed along the fault, thought to have a major strike-slip component. Tunneling revealed that the feature was actually a pair of relatively small, northwest-striking, vertical faults about 5 meters apart. In the ESF, the trace of the fault is observed as two subparallel northwest-striking faults approximately 1900 m from the north tunnel portal. These faults produce a total west-side down offset of about 4 m in the ESF but have subhorizontal slickenlines that indicate a right-lateral sense of offset.

A southwestern strand of the Drill Hole Wash fault runs beneath the center of the wash northwest of the ESF North Ramp; it is exposed in bedrock northwest of the northern turn of the ESF [4]. At this location, the Tiva Canyon Tuff is displaced 15 m down-to-the-southwest by several discontinuous fault splays; the amount of stratigraphic throw decreases abruptly in both directions from these outcrops and evidently ceases before reaching the tunnel.

Fractures

At the scale of 10 to 50 meters, the fracture network and faults with small displacements are the principal observable structural elements. The fracture network subdivides the mountain into innumerable fracture-bounded blocks and forms a pervasive mesoscopic fabric element. Cooling fractures act as a significant pre-existing weakness in the rock mass and are the principal control on the style of deformation at this observational scale. Each lithostratigraphic zone has its own characteristic suite of fracture attributes, including fracture orientation, spacing, and trace length. These differences result in a stratigraphic control of rock-mass mechanical properties and structural geometry.

Fracture Types

Cooling fractures are smooth, gently curved to planar discontinuities that are inferred to have formed early in the history of the volcanic rock mass, in response to localized stresses during the cooling and crystallization of the tuff. Cooling fractures were initially identified from the presence of tubular structures on the fracture surface and very low roughness coefficients [71, 80]. A combination of other criteria have been used successfully to identify probable cooling fractures where tubular structures are absent [81], including: low surface roughness; smooth, continuous traces; great length relative to other fractures; parallelism with proven cooling fractures nearby; presence of demonstrated early age as shown through abutting relations with fractures of other sets; and the presence of vapor-phase rinds composed of minerals that formed at high temperatures.

Cooling fractures within the Topopah Spring and Tiva Canyon Tuffs often consist of two orthogonal sets that are steeply dipping, and, less commonly, a third, subhorizontal set. The fracture orientations combine in three dimensions to form primarily rhombohedral shapes in most lithologic units and crude hexagonal columnar shapes in the lower parts of the crystallized Tiva Canyon and Topopah Spring Tuffs.

Tectonic fractures are discontinuities that have formed in response to regional tectonic stresses or local stresses. Tectonic stresses may also reactivate previously formed cooling joints. Abundant tectonic fractures are present at Yucca Mountain apart from those formed during cooling and, in some cases, these structures have reactivated pre-existing cooling fractures. These fractures tend to have more scattered orientation distributions, tend to be shorter and rougher, and generally lack vapor-phase mineralization on their surfaces. Tectonic fractures terminate against older discontinuities such as cooling fractures or vapor-phase partings and thus are developed within the larger blocks formed by the cooling fractures. Based upon mapped termination relations, and fracture reactivation and offset relations, Throckmorton and Verbeek [81] interpreted subvertical north-striking, northwest-striking, and northeast-striking tectonic fracture sets at Yucca Mountain to have developed sequentially as a response to distinct phases of regional extension. Subsequent mapping at the surface and underground has documented greater variability in orientations and less distinct termination relations, suggesting that north-striking and northwest-striking fractures may have developed at the same time, rather than sequentially.

Since nonwelded units do not generally form cooling fractures, all discontinuities displayed within such units are tectonic. Because the nonwelded units are generally much softer and less brittle than the densely welded rocks, the same stresses that developed tectonic fractures and reactivated cooling fractures in the welded units formed minor faults with intermediate dips in nonwelded units. These features generally have no aperture and infillings are limited to thin (less than 1 cm thick) zones of comminuted wall rock.

Lithostratigraphic Controls on Fracture Geometry

Variations in lithology across depositional boundaries and variations in welding, crystallization and lithophysae development within welded ignimbrites of the Paintbrush Group control fracture network properties such as intensity and network connectivity. Such lithostratigraphic controls result in markedly stratabound fractures within the Paintbrush Group (Fig. 7).

Fracture characteristics in the ignimbrites at Yucca Mountain are primarily controlled by variations in welding. Welded flow units of the Tiva Canyon and Topopah Spring Tuffs are observed in boreholes to have higher fracture frequencies than the nonwelded units within the Paintbrush Group and the underlying Calico Hills Formation [32, 33, 37, 38, 82]. Surface mapping also shows that fracture intensity and network connectivity within nonwelded and poorly welded units are much lower than in the surrounding welded units [77]. Fracture intensity increases with degree of welding within the ignimbrites due to the presence of cooling fractures and because increasing brittleness of the rock favors an increase in the number of tectonic fractures. The welding transitions such as those at the base of the Tiva Canyon Tuff and the top of the Topopah Spring Tuff are also transitional in their fracture intensities. Both cooling and tectonic fractures often terminate abruptly at these welding transitions (Fig. 7).

Within the crystallized, densely welded units, fracture intensity also varies with the abundance of lithophysal cavities (Fig. 8). Where lithophysae are abundant, the frequency of map-scale (1-m or longer) fractures drops proportionally; conversely, where lithophysae decrease in size and abundance, map-scale fractures increase. For example, the middle nonlithophysal zone of the Topopah Spring Tuff (Tptpmn) generally is moderately fractured, exhibiting map-scale fracture densities of 4 to 6 fractures per meter (Fig. 9F). Within a meter of the contact with the underlying lower lithophysal zone (Tptpll), fracture density drops to less than one fracture per meter (Fig. 8). Numerous well-developed cooling and tectonic fractures can be traced down the ESF tunnel wall to the Tptpmn/Tptpll contact, where they usually terminate within a meter of the contact. Data from the Cross Drift indicate that in the upper and lower lithophysal zones of the Topopah Spring Tuff, throughgoing fractures are rare where the percentage of lithophysae exceeds 10 percent.

The change in the style of fracturing in rocks that have undergone essentially the same stresses and have similar characteristics, except lithophysal percentage, lead to the conclusion that lithophysae must serve to attenuate a fracture's ability to propagate through the rock mass. In addition to a decrease in fracture intensity, fracture sets frequently terminate or change orientation at or near the boundaries of lithophysal zones. Where lithophysae are present in the rock, cooling fractures intersect few of them. These changes in orientation and character points to the pre-existence of the lithophysae prior to cooling fracture formation [71].

Although lacking numerous map-scale fractures, lithophysal zones are characterized by locally intense fractures shorter than 1 m in length. Fracture-trace-length distributions at Yucca Mountain suggest that fracture size and abundance are related and may be approximated by power-law or exponential distributions [71, 77]. Consequently, a large number of short-trace-length fractures simply fall below the mapping cutoff of 1 m but represent a continuum of fractures with the larger, mapped features. In addition, lithophysae-bearing zones possess a short-trace-length fracture fabric that does not appear to have a counterpart in the map-scale features. Fractures in these zones range in length from a few centimeters to a few decimeters and typically occur as radiating patterns of fractures that occupy necks between lithophysal cavities or that nucleate from lithophysae tips or irregularities [83].

Fracture characteristics of stratigraphic units at Yucca Mountain

The Tiva Canyon Tuff is characterized by a pervasive network of cooling and tectonic fractures. Cooling fractures in the crystal-poor upper lithophysal zone and the crystal-rich member are large, steeply dipping, and often form two orthogonal sets. Fractures in the underlying middle nonlithophysal zone are more numerous, but are shorter, forming an anastamosing network of curved fractures.

Fractures within the stratigraphic units of the PTn hydrogeologic unit are much less pervasive than in the surrounding welded units. Most fractures are stratabound and terminate at lithologic contacts. Fractures are widely and irregularly spaced, except within the welding transitions that define the upper and lower contacts of the PTn unit (e.g., at the base of the Tiva Canyon Tuff). Numerous small faults are observed in this interval, both at the surface and in the ESF. Most faults are narrow, sharp breaks, with no attendant brecciation or fracturing.

Similar to the Tiva Canyon Tuff, the Topopah Spring Tuff has a well-developed network of cooling and tectonic fractures. Especially in the middle nonlithophysal zone, long cooling fractures of various orientations are common. As discussed above, most of the long cooling fractures in the middle nonlithophysal zone terminate abruptly at the contact with the underlying lower lithophysal zone (Fig. 7). Similar to the Tiva Canyon Tuff, numerous faulted fractures with small displacements are observable in the Topopah Spring Tuff. However, little brecciation along fracture surfaces or distributed brecciation is observed within the Topopah Spring Tuff. Fault zones at the level of the Topopah Spring Tuff are narrow. The zone of fault-related fracturing and brecciation is typically only a few meters wide.

A significant feature occurring in the middle nonlithophysal zone of the Topopah Spring Tuff is the presence of an intensely fractured zone (IFZ) located along the Main Drift of the ESF. The zone, as encountered in the ESF, is nearly 950 m wide and composed almost entirely of steeply dipping, cooling joints spaced 2-6 cm apart (Fig. 9G), oriented along a single orientation – N 30° to 55° W. Fracture densities measured by traceline surveys through this zone exceed 12 fractures/meter in some areas. The IFZ is significant because it represents a substantial interval of discontinuities that may influence the hydrologic, pneumatic, thermal-mechanical, or construction conditions at Yucca Mountain. The zone has not been observed in the overlying Tiva Canyon Tuff. Fracture data from borehole video in near vertical boreholes across the central block area show that the middle nonlithophysal zone of the Topopah Spring Tuff has generally high fracture frequencies, but that the intervals of closely-spaced, steeply-dipping fractures are confined to the middle nonlithophysal zone. Local zones of closely spaced northwest-striking fractures are present in outcrops of the middle nonlithophysal zone of the Topopah Spring Tuff in Solitario Canyon, but are much less continuous than the IFZ intersected by the ESF. The origin of this joint zone is enigmatic. The IFZ corresponds spatially to the interval of greatest offset along the Ghost Dance fault [76], suggesting possible structural control. The northern boundary of the IFZ appears to correspond to southern limit of a lithophysae-bearing subzone within the middle nonlithophysal zone of the Topopah Spring Tuff, allowing the suggestion of lithostratigraphic control of fracture density [56]. However, no satisfactory explanation has been proposed that accounts for the fracture intensity, consistency in fracture orientation and great width of the zone.

SUMMARY

The geologic system at Yucca Mountain forms a fundamental framework for understanding the performance of the site as a potential geologic repository for high-level radioactive waste. During the course of site characterization at Yucca Mountain, a large amount of geologic data has been collected including geologic map data, stratigraphic information from boreholes, and structural characterization of the site at a variety of scales both at the surface and in the subsurface. The stratigraphy, structure, and rock material properties of the site play a fundamental role in defining model parameters in hydrologic flow and transport models of both the unsaturated and saturated zones. Lithologic properties such as the degree of welding, crystallization, lithophysae development, and alteration control rock matrix porosity and permeability and ultimately play a role in predictions of groundwater travel time. The original distribution of devitrified and vitric tuffs have largely determined the patterns of alteration (especially zeolitic alteration), which in turn bears on the potential for sorption of radionuclides that migrate through the unsaturated zone. Faults may serve as conduits or barriers to fluid flow; connectivity of structural features bear on the number and length of fluid pathways. Fracture data at Yucca Mountain are used in models of surface infiltration, numerical simulations of discrete fracture networks, and bulk-rock permeability calculations for equivalent continuum models of the unsaturated zone.

Engineering design of the proposed repository relies heavily on lithologic and structural characteristics of the rock. The distribution of faults and their observed character (width, offset, damage to adjacent rock mass) at the surface and underground has played a role in considerations of the repository footprint and total volume. Understanding fault zone and fracture network properties is important for characterizing the mechanical stability of the potential repository and for estimating the amount of ground support needed in underground construction. Mechanical and structural characteristics of lithostratigraphic units, such as rock strength, fracture intensity, fracture aperture, and fracture infilling all partly determine how the site would respond to the emplacement of nuclear waste and the conditions that would be imposed on the rock by such emplacement.

Acknowledgements -

The authors wish to thank technical reviewers Robert Dickerson and Tom Moyer whose considerable efforts resulted in dramatic improvements to a draft of this manuscript. The authors also wish to acknowledge the continuing exceptional work of photographer David W. Wehner, TRW Safety Systems, Inc. who provided all of the photographs in this paper, except photo 3, which was taken by the authors.

Much of the site characterization data produced on the Yucca Mountain Project is contained exclusively in internal reports and U.S. Geological Survey Administrative Reports.

Much of this information can be accessed by the public via the Internet at www.ymp.gov. Hard copies of various reports can be accessed by contacting the Department of Energy, Institutional Affairs, at 1551 Hillshire Drive, Las Vegas, NV, 89134.

REFERENCES

1. Barton, N., Lien, R., and Lunde, J., Engineering Classification of Rock Masses for the Design of Tunnel Support. *Rock Mechanics* 6, 1975, pp. 183-236
2. Bieniawski, Z.T., Rock Mass Classifications in Rock Engineering. *Exploration for Rock Engineering,* ed. Z.T. Bieniawski, A.A. Balkema, Johannesburg, 1976, pp. 97-106.
3. Bieniawski, Z.T, The Geomechanics Classification in Rock Engineering Applications. *Proceedings 4th International Congress of Rock Mechanics,* ISRM, Montreux, vol. 2, 1979, pp. 41-48.
4. Day, W.C., Potter, C.J., Sweetkind, D.S., Dickerson, R.P., and San Juan, C.J., Bedrock geologic map of the Central Block area, Yucca Mountain, Nye County, Nevada. *U.S. Geological Survey Miscellaneous Investigations Series I-2601*, 1:6000 scale, 1998, 2 plates with text.
5. Carr, W.J., Regional structural setting of Yucca Mountain, southeastern Nevada, and late Cenozoic rates of tectonic activity in part of the southwestern Great Basin, Nevada and California. *U.S. Geological Survey Open-File Report 84-854*, 1984, 98 p.
6. Wernicke, B.P., Axen, G.J., and Snow, J.K., Basin and Range extensional tectonics at the latitude of Las Vegas, Nevada. *Geological Society of America Bulletin*, v. 100, 1988, p. 1738-1757.
7. Stewart, J.H., Tectonics of the Walker Lane Belt, western Great Basin—Mesozoic and Cenozoic deformation in a zone of shear. I*n* Ernst, W.G., ed., *Metamorphism and crustal evolution of the western United States*, Rubey volume: Englewood Cliffs, New Jersey, Prentice Hall, 1988, p. 683-713.

8. Carr, W.J., Styles of extension in the Nevada Test Site region, southern Walker Lane Belt. An intergration of volcano-tectonic and detachment fault models *in* Wernicke, B. P., ed., Basin and Range extensional tectonics near the latitude of Las Vegas, Nevada. *Geological Society of America Memoir 176*, 1990, p. 283-303.

9. Fridrich, C.J., Tectonic evolution of Crater Flat basin, Yucca Mountain, Nevada. *in* Wright. L. A., and Troxel, B. W., eds., Cenozoic Basins of the Death Valley Region. *Geological Society of America Special Paper 333*, Boulder, Colorado, 1999, p.169-195.

10. Brocher, T.M., Hunter, W.C., and Langenheim, V.E., Implications of seismic reflection and potential field geophysical data on the structural framework of the Yucca Mountain-Crater Flat region, Nevada. *Geological Society of America Bulletin*, v. 110, 1998, p. 947-971.

11. Monsen, S. A., Carr, M. D., Reheis, M. C., and Orkild, P. P., Geologic Map of Bare Mountain, Nye County, Nevada. *U.S. Geological Survey Miscellaneous Investigations Series map I-2201*, scale 1:24,000, with text, 1992, 6 p.

12. Winograd, I.J. and Thordarson, W., Hydrogeologic and hydrochemical framework, south-central Great Basin, Nevada-California, with special reference to the Nevada Test Site. *U.S. Geological Survey Professional Paper 712-C*, 1975,126 p, 3 plates.

13. Sawyer, D.A. Fleck, R.J., Lanphere, M.A., Warren, R.G., and Broxton, D.E., Episodic volcanism in the Miocene southwest Nevada volcanic field—Stratigraphicfield—Stratigraphic revisions, $^{40}Ar/^{39}Ar$ geochronologic framework, and implications for magmatic evolution. *Geological Society of America Bulletin,* v. 106, 1994, p. 1304-1318.

14. Byers, F.M., Jr., Carr, W.J., Orkild, P.P., Quinlivan, W.D., and Sargent, K.A., Volcanic suites and related cauldrons of the Timber Mountain-Oasis Valley Caldera Complex, southern Nevada. *U.S. Geological Survey Professional Paper 919*, 1976, 70 p.

15. Byers, F.M., Jr., Carr, W.J., and Orkild, P.P., Volcanic centers of southwestern Nevada — evolution of understanding, 1960-1988. *Journal of Geophysical Research*, v. 94, 1989, p. 5908-5924.

16. Carr, W.J., Byers, F.M., Jr., and Orkild, P.P., Stratigraphic and volcano-tectonic relations of the Crater Flat Tuff and some older volcanic units, Nye County, Nevada. *U.S. Geological Survey Professional Paper 1323*, 1986, 28 p.

17. Ferguson, J.F., Cogbill, A.H., and Warren, R.G., A geophysical-geological transect of the Silent Canyon caldera complex, Pahute Mesa, Nevada. *Journal of Geophysical Research*, v. 99, 1994, p. 4323-4339.

18. Lipman, P.W., Christiansen, R.L., and O'Connor, J.T., A compositionally zoned ash-flow sheet in southern Nevada. *U.S. Geological Survey Professional Paper 524-F*, 1966, 47 p.

19. Spengler, R.W., and Fox, K.F., Jr., Stratigraphic and structural framework of Yucca Mountain, Nevada. *in Radioactive waste management and the nuclear fuel cycle,* v. 13(1-4), 1989, p. 21-36.

20. Carr, M.D., Waddell, S.J., Vick, G.S., Stock, J.M., Monsen, S.A., Harris, A.G., Cork, B.W., and Byers, F.M., Jr., Geology of drill hole UE-25p#1: A test hole into pre-Tertiary rocks near Yucca Mountain, southern Nevada. *U.S. Geological Survey Open-File Report 86-175,* 1986, 87 p.

21. Scott, R.B., and Bonk, J., Preliminary geologic map of Yucca Mountain, Nye County, Nevada, with geologic sections. *U.S. Geological Survey Open-File Report 84-494*, 1:12,000 scale, 1984, 2 sheets.

22. Day and others, Day, W.C., Dickerson, R.P., Potter, C.J., Sweetkind, D.S., San Juan, C.A., Drake, R.M., II, and Fricdrich, C.J., Bedrock geologic map of the Yucca Mountain area, Nye County, Nevada. *USGS Geologic Investigations Map I-2627,* 1:24,000 scale, 1998, 1 plate with text.

23. Hevesi, J.A., Flint, A.L., ans Istok, J.D., Precipitation estimation in mountainous terrain using multivariate geostatistics. Part II: isohyetal maps. *Journal of Applied Meterology,* v. 31, 1993, p. 677-688.

24. Rousseau, J.P., Kwicklis, E.M., and Gilles, D.C., (eds), Hydrogeology of the Unsaturated Zone, North Ramp Area of the Exploratory Studies Facility, Yucca Mountain, Nevada, USGS-WRIR-98-4050, *Water-Resources Investigations Report, U.S. Geological Survey,* Denver, Colorado, 1999, p. 43-64.

25. Luckey, R.R., Tucci, Patrick, Faunt, C.C., and Ervin, E.M., Status of understanding of the saturated-zone ground-water flow system at Yucca Mountain, Nevada, as of 1995. *U.S. Geological Survey Water Resource Investigation Report 96-4077*, 1996, 14 p.

26. Tucci, Patrick, and Burkhardt, D.J., Potentiometric-surface map, Yucca Mountain and vicinity, Nevada. *U.S. Geological Survey Open-File Report 95-4149*, 1995, 15 p.

27. Fridrich. C.J., Dudley, W.W., and Stuckless, J.S., Hydrogeologic analysis of the saturated-zone ground-water system, under Yucca Mountain, Nevada. *Journal of Hydrology,* v. 154, 1994, p. 133-168.

28. Czarnecki, J.B., O'Brien, G.M., Nelson, P.H., Is there perched water under Yucca Mountain in Borehole USW G-2?. *American Geophysical Union Transactions Fall Meeting Abstracts and Programs, v. 75,* no. 44, 1994, p. 249-250.

29. Ervin, E.M., Luckey, R.R., and Burkhardt. D.J., Revised potentiomentric-surface map, Yucca Mountain and vicinity, Nevada. *U.S. Geological Survey Water-Resources Investigations Report 93-4000,* 1994, 17 p.

30. Montazer, P. and Wilson, W.E., Conceptual hydrologic model of flow in the unsaturated zone, Yucca Mountain, Nevada. *U.S. Geological Survey Water Resources Investigation Report 84-4345*, 1984, 55 p.

31. Spengler, R. W., Byers, F.M., Jr., and Warner, J.B., Stratigraphy and structure of volcanic rocks in drill hole USW G-1, Yucca Mountain, Nye County, Nevada. *U.S. Geological Survey Open File Report 81-1349*, 1981, 50 p., 1 plate.

32. Spengler, R.W., Chornack, M.P., Muller, D.C., and Kibler, J.E., Stratigraphic and structural characteristics of volcanic rocks in core hole USW G-4, Yucca Mountain, Nye County, Nevada. *U.S. Geological Survey Open-File Report 84-789,* 1984, 77 p.

33. Scott, R.B., and Castellanos, M., Stratigraphic and structural relations of volcanic rocks in drill holes USW GU-3 and USW G-3, Yucca Mountain, Nye County, Nevada. *U.S. Geological Survey Open File Report 84-491*, 1984, 121 p.

34. Geslin, J.K., and Moyer, T.C., Summary of lithologic logging of new and existing boreholes at Yucca Mountain, Nevada, March 1994 to June 1994. *U.S. Geological Survey Open-File Report 94-451*, 1995, 16 p.

35. Geslin, J.K., Moyer, T.C., and Buesch, D.C., Summary of lithologic logging of new and existing boreholes at Yucca Mountain, Nevada, August 1993 to February 1994. *U.S. Geological Survey 94-342*, 1995, 39 p.

36. Moyer, T.C., and Geslin, J.K., Lithostratigraphy of the Calico Hills Formation and Prow Pass Tuff (Crater Flat Group) at Yucca Mountain, Nevada. *U.S. Geological Survey Open-File Report 94-460*, 1995, 59 p.

37. Rautman, C.A., and Engstrom, D.A., Geology of the USW SD-12 Drill Hole, Yucca Mountain, Nevada. *Sandia National laboratories Report SAND96-1368*, 1996, 131 p.

38. Rautman, C.A., and Engstrom, D.A., Geology of the USW SD-7 Drill Hole, Yucca Mountain, Nevada. *Sandia National laboratories Report SAND96-1474*, 1996, 163 p.

39. Buesch, D.C., Spengler, R.W., Moyer, T.C., and Geslin, J.K., Proposed stratigraphic nomenclature and macroscopic identification of lithostratigraphic units of the Paintbrush Group exposed at Yucca Mountain, Nevada. *U.S. Geological Survey Open-File Report 94-469*, 1996, 45 p.

40. Moyer, T.C., Geslin, J.K., and Flint, L.E., Stratigraphic relations and hydrologic properties of the Paintbrush Tuff nonwelded (PTn) hydrologic unit, Yucca Mountain, Nevada. *U.S. Geological Survey Open-File Report 95-397*, 1996, 151 p.

41. Buesch, D.C., and Spengler, R.W., Stratigraphic framework of the North Ramp Area of the Exploratory Studies Facility, Yucca Mountain, Nevada. *in* Rousseau, J.P., Kwicklis, E.M., and Gilles, D.C., (eds), Hydrogeology of the Unsaturated Zone, North Ramp Area of the Exploratory Studies Facility, Yucca Mountain, Nevada, USGS-WRIR-98-4050, *Water-Resources Investigations Report, U.S. Geological Survey,* Denver, Colorado, 1999, p. 43-64.

42. Buesch, D.C., and Spengler, R.W., 1999, Correlations of lithostratigraphic features with hydrogeologic properties, a facies-based approach to model development in volcanic rocks at Yucca Mountain, Nevada. in Slate, J.L., ed., *Proceedings of Conference on Status of Geologic Research and Mapping, Death valley National Park, U.S. Geological Survey Open-File Report 99-153*, p. 62-64.

43. Moyer, T.C., Geslin, J.K., and Buesch, D.S., Summary of lithologic logging of new and existing boreholes at Yucca Mountain, Nevada, July 1994 to November 1994. *U.S. Geological Survey Open-File Report 95-102*, 1995, 27 p.

44. Flint, L.E., Characterization of hydrogeologic units using matrix properties, Yucca Mountain, Nevada. *U.S. Geological Survey Water-Resources Investigations Report WRIR97-4243*, 1998, 64 p.

45. Ortiz, T.S., Williams, R.L., Nimick, F.B., and South, D.L., Three-dimensional model of reference thermal/mechanical and hydrological stratigraphy at Yucca Mountain, southern Nevada. *Sandia National Laboratories Report SAND-84-1076*, 1985, 80 p.

46. Bodvarsson, G.S.; Bandurraga, T.M.; and Wu, Y.S. (Eds.) The Site-Scale Unsaturated Zone Model of Yucca Mountain, Nevada, for the Viability Assessment. *LBNL-40376*. Berkeley, California: Lawrence Berkeley National Laboratory. 1997.

47. Nelson, P.H., Computation of porosity and water content from geophysical logs, Yucca Mountain, Nevada. *U.S. Geological Survey Open-File Report 96-078*. 1996, 64 p.

48. Nelson, P.H., Muller, D.C., Schimschal, U., and Kilber, J.E., Geophysical logs and core measurements from forty boreholes at Yucca Mountain, Nevada. *U.S. Geological Survey Geophysical Investigations Map GP-1001,* 1991, 64 p.

49. Buesch, D.C., and Spengler, R.W., Detailed correlation of lithostratigraphic and borehole geophysical log data for identifying contacts at Yucca Mountain. *in International High-Level Radioactive Waste Management Conference, American Nuclear Society,* Le Grange Park, Illinois, 1998, p. 248-251.

50. Buesch, D.C., Spengler, R.W., Nelson, P.H., and Flint, L.E., Correlation of lithologic features, hydrogeologic properties, and borehole geophysical logs at Yucca Mountain, Nevada. *Geological Society of America, Boulder, Colorado, Abstracts with Programs*, v. 28, no. 7, 1996, p. A-521.

51. Smith, R.L., Ash flows. *Geological Society of America Bulletin, v. 71*, 1960, p. 795-842.

52. Smith, R.L., Zones and zonal variations in welded tuffs. *U.S. Geological Survey Professional Paper 354-F*, 1960, p. 149-159.

53. Sheridan, M.F., and Ragan, D.M., Compaction of ash-flow tuffs, *in* Chilingarian, G.V., and Wolf, K.H., ed., Compaction of coarse-grained sediments, II; *Developments in Sedimentology 18B.* Amsterdam, Elsevier, 1977, p. 677-713.

54. Ross, C.S., and Smith, R.L., Ash-flow tuffs: their origins, geologic relations and identification. *U.S. Geological Survey Professional Paper 366*, 1961, p. 1-77.

55. Bish, D.L., and Chipera, S.J., Revised mineralogic summary of Yucca Mountain, Nevada. *Los Alamos National Laboratory Report LA-11497-MS*, 1989, 68 p.

56. Buesch, D.C., and Spengler, R.W., Character of the middle nonlithophysal zone of the Topopah Spring Tuff at Yucca Mountain. *in International High-Level Radioactive Waste Management Conference, American Nuclear Society,* Le Grange Park, Illinois, 1998, p. 248-251.

57. Buesch, D.C., Beason, S.C., and Spengler, R.W., Relations among welding, vapor-phase activity, crystallization, and fractures in the Tiva Canyon and Topopah Spring Tuffs at Yucca Mountain, Nevada. *Geological Society of America, Boulder, Colorado, Abstracts with Programs*, v. 31, no. 7, 1999, p. A476-A477.

58. Vaniman, D.T., Bish, D.; Broxton, D., Byers, F., Heiken, G., Carlos, B., Semarge, E., Caporuscio, F., and Gooley, R.. Variations in Authigenic Mineralogy and Sorptive Zeolite Abundance at Yucca Mountain, Nevada, Based on Studies of Drill Cores USW GU-3 and G-3. *LA-9707-MS.* Los Alamos, New Mexico, Los Alamos National Laboratory, 1984.

59. Peterman, Z.E., Spengler, R.W., Singer, F.R., and Beason, S.C., Localized Alteration of the Paintbrush Nonwelded Hydrologic Unit within the Exploratory Studies Facility. *High Level Radioactive Waste Management, Proceedings of the Seventh Annual International Conference, Las Vegas, Nevada, April 29-May 3,* 1996, p. 46-47.

60. Levy, S.S., Surface-Discharging Hydrothermal Systems at Yucca Mountain--Examining the Evidence. *In Scientific Basis for Nuclear Waste Management XVI, Interrante*, C.G. and Pabalan, R.T., (eds.) *Materials Research Society Symposium Proceedings,* v. 294, Pittsburgh, Pennsylvania: Materials Research Society, 1993, p. 543-548.

61. Broxton, D.E., Bish, D.L., and Warren, R.G., Distribution and chemistry of diagenetic minerals at Yucca Mountain, Nye County, Nevada. *Clays and Clay Minerals,* v. 35, no. 2, 1987, pp. 89-110.

62. Broxton, D.E., Warren, R.G., Hagan, R.C., and Luedemann, G. Chemistry of Diagenetically Altered Tuffs at a Potential Nuclear Waste Repository, Yucca Mountain, Nye County, Nevada. *LA-10802-MS.* Los Alamos, New Mexico: Los Alamos National Laboratory, 1986, 160 p.

63. Johnstone, J.K. and Wolfsberg, K., (eds.) Evaluation of tuff as a medium for a nuclear waste repository: Interim status report on the properties of tuff. *Sandia National Laboratories Report SAND80-1464*, 1980, 134 p.

64. Scott, R.B., Tectonic setting of Yucca Mountain, southwest Nevada. In Wernicke, B.P., (ed.), Basin and Range extensional tectonics near the latitude of Las Vegas, Nevada. *Geological Society of America Memoir 176,* 1990, p. 251-282

65. Simonds, F.W., Whitney, J.W., Fox, K.F., Ramelli, A.R., Yount, J.C., Carr, M.D., Menges, C.M., Dickerson, R.P., and Scott, R.B., Map showing fault activity in the Yucca Mountain area, Nye County, Nevada. *U.S. Geological Survey Miscellaneous Investigations Series I—2520,* 1:24,000 scale, 1995, 1 sheet.

66. Swadley, W. C., D. L. Hoover, and J. N. Rosholt, Preliminary Report on Late Cenozoic Faulting and Stratigraphy in the Vicinity of Yucca Mountain, Nye County, Nevada. *U.S. Geologic Survey Open-File Report 84-788,* Map Scale 1:62,000, 1984, 42 pp

67. Taylor, E.M. and Huckins, H.E., Lithology, fault displacement, and origin of secondary calcium carbonate and opaline silica at trenches 14 and 14D on the Bow Ridge fault at Exile Hill, Nye County, Nevada. *U.S. Geological Survey Open-File Report 93-477,* 1995, 38 p., 1 plate.

68. Hudson, M.R., Sawyer, D.A., and Warren, R.G., Paleomagnetism and rotation constraints for the middle Miocene southwestern Nevada volcanic field. *Tectonics,* v. 13, no. 2, 1994, p. 258-277.

69. Minor, S.A., Hudson, M.R., and Fridrich, C.J., Fault-slip data, paleomagnetic data, and paleostress analyses bearing on the Neogene tectonic evolution of northern Crater Flat

basin, Nevada. *U.S. Geological Survey Open-File Report 97-285,* 1997, 41 p. plus appendices.

70. Potter, C.J., Dickerson, R.P., and Day, W.C., Nature and continuity of the Sundance Fault, Yucca Mountain, Nevada. *U.S. Geological Survey Open-File Report 98-266*, scale 1:2,400, 1999, 3 plates with text.

71. Barton, C.C., Larsen, E., Page, W.R., and Howard, T.M., Characterizing fractured rock for fluid-flow, geomechanical, and paleostress modeling. Methods and preliminary results from Yucca Mountain, Nevada. *U.S. Geological Survey Open-File Report 93-269*, 1993, 62 p.

72. Potter, C.J., Day, W.C., Sweetkind, D.S., and Dickerson, R.P., Fault styles and strain accommodation in the Tiva Canyon Tuff, Yucca Mountain, Nevada. *EOS, Transactions, American Geophysical Union,* v. 77, no. 17, 1996, p. S265.

73. Sweetkind, D.S., Potter, C.J., and Verbeek, E.R, Interaction between faults and the fracture network at Yucca Mountain, Nevada. *EOS, Transactions, American Geophysical Union,* v. 77, no. 17, 1996, p. S266.

74. Buesch, D.C., Dickerson, R.P., Drake, R.M., and Spengler, R.W., Integrated geology and preliminary cross section along the north ramp of the Exploratory Studies Facility, Yucca Mountain. In *High level radioactive waste management, Proceedings of the Fifth Annual International Conference: Las Vegas, Nevada*, May 22-26, 1994, American Nuclear Society, Inc. and American Society of Civil Engineers, v. 2, 1994, p. 1055-1065.

75. Potter, C.J., Day, W.C., San Juan, C., Sweetkind, D.S., and Drake R.M., II, Pre-construction geologic section along the Cross Drift through the potential high-level radioactive waste repository, Yucca Mountain, Nye County, Nevada. *U.S. Geological Survey Open File Report 98-530*, 1998, 22 p., 1 plate.

76. Spengler, R.W., Braun, C.A., Linden, R.M., Martin, L.G., Ross-Brown, D.M., and Blackburn, R.L., Structural character of the Ghost Dance fault, Yucca Mountain, Nevada. In *High Level Radioactive Waste Management Proceedings of the Fourth International Conference, American Nuclear Society,* v. 1., 1993, pp. 653-659

77. Sweetkind, D.S., Williams-Stroud, S., and Coe, J., Characterizing the fracture network at Yucca Mountain, Nevada, Part 1. Integration of field data for numerical simulations. in, Hoak, T.E., Klawitter, A.L., and Blomquist, P.K., eds., Fractured Reservoirs: Characterization and Modeling. *Rocky Mountain Association of Geologists 1997 Guidebook,* 1997, p. 185-196.

78. Spengler, R.W., Braun, C.A., Martin, L.G., and Weisenberg, C.W., The Sundance fault—a newly recognized shear zone at Yucca Mountain, Nevada. *U.S. Geological Survey Open-File Report 94-49*, 1994, 11 p.

79. Spengler, R.W., and Rosenbaum, J.G., Preliminary interpretations of geologic results obtained from boreholes UE25a-4, -5, -6, and -7, Yucca Mountain, Nevada Test Site. *U.S. Geological Survey Open-File Report 80-929*, 1980, 33 p.

80. Barton, C.C., Howard, T.M., and Larsen, E., Tubular structures on the faces of cooling fractures - A new volcanic feature. *EOS, Transactions of the American Geophysical Union,* v. 65, 1984, p. 1148.

81. Throckmorton, C.K., and Verbeek, E.R., Fracture networks in the Tiva Canyon and Topopah Spring Tuffs of the Paintbrush Group, southwestern Nevada. *U.S. Geological Survey Open File Report 95-2*, 1995, 179 pp.

82. Engstrom, D.A., and Rautman, C.A., Geology of the USW SD-9 Drill Hole, Yucca Mountain, Nevada. *Sandia National laboratories Report SAND96-2030,* 1996, 128 p.

83. Sweetkind, D.S., Rautman, C.A., and Singleton, W.L., Evaluation of Short-Trace-Length Fractures at Yucca Mountain, Nevada. *EOS, Transactions, American Geophysical Union,* 79, 1998, p. S231.

84. Chipera, S.J., Vaniman, D.T., Carlos, B.A., and Bish, D.L., Mineralogic variation in drill core UE-25 UZ#16, Yucca Mountain, Nevada. *Los Alamos National Laboratory Report LA-12810-MS*, 1995, 40 p.

FIGURES

Figure 5 Lithophysae, spots, streaks, veinlets, stringers, and vapor-phase partings in the Topopah Spring Tuff. A) Components of lithophysae, streaks, veinlets, stringers, and vapor-phase partings [39]. B) Photograph of cm-sized lithophysae in the upper lithophysal zone in the ESF. C) Photograph of the contact of the upper lithophysal and middle nonlithophysal zone (Tptpul-Tptpmn) that includes dm- and cm-sized lithophysae, cm-sized spots, vapor-phase partings, and groundmass. D) Close up photograph of an anastamosing vapor-phase parting from the middle nonlithophysal zone.

Figure 6 Lithostratigraphic units and thermal-mechanical data from borehole NRG-6. Lithostratigraphic zones are labeled as in Figure 3.

Figure 7 Diagrammatic cross section of the Topopah Spring Tuff illustrating general distribution of fractures, faults, and lithophysae within the ignimbrite.

Figure 8 Fracture density and lithophysal abundance along the Cross Drift. Fracture frequency is shown as number of 1-m and longer fractures per meter, averaged over 10-m intervals.

Figure 9 E) View looking south along the crest of Yucca Mountain toward Amargosa Valley. The Tiva Canyon Tuff comprises the majority of the lithostratigraphic units exposed on the surface of Yucca Mountain and forms the cliff in the foreground. The Solitario Canyon fault bounds the west side of Yucca Mountain (upper center of photo). F) View of the excavation for the Heated Drift Test in the Topopah Spring Tuff, crystal-poor, middle nonlithophysal zone. Note high-angle fractures in the floor of the drift, and intermediate angle shears in the face. G) Close up of cooling fractures in the Intensely Fractured Zone. This tight spacing extends along the Main Drift of the ESF for nearly 1000 m.

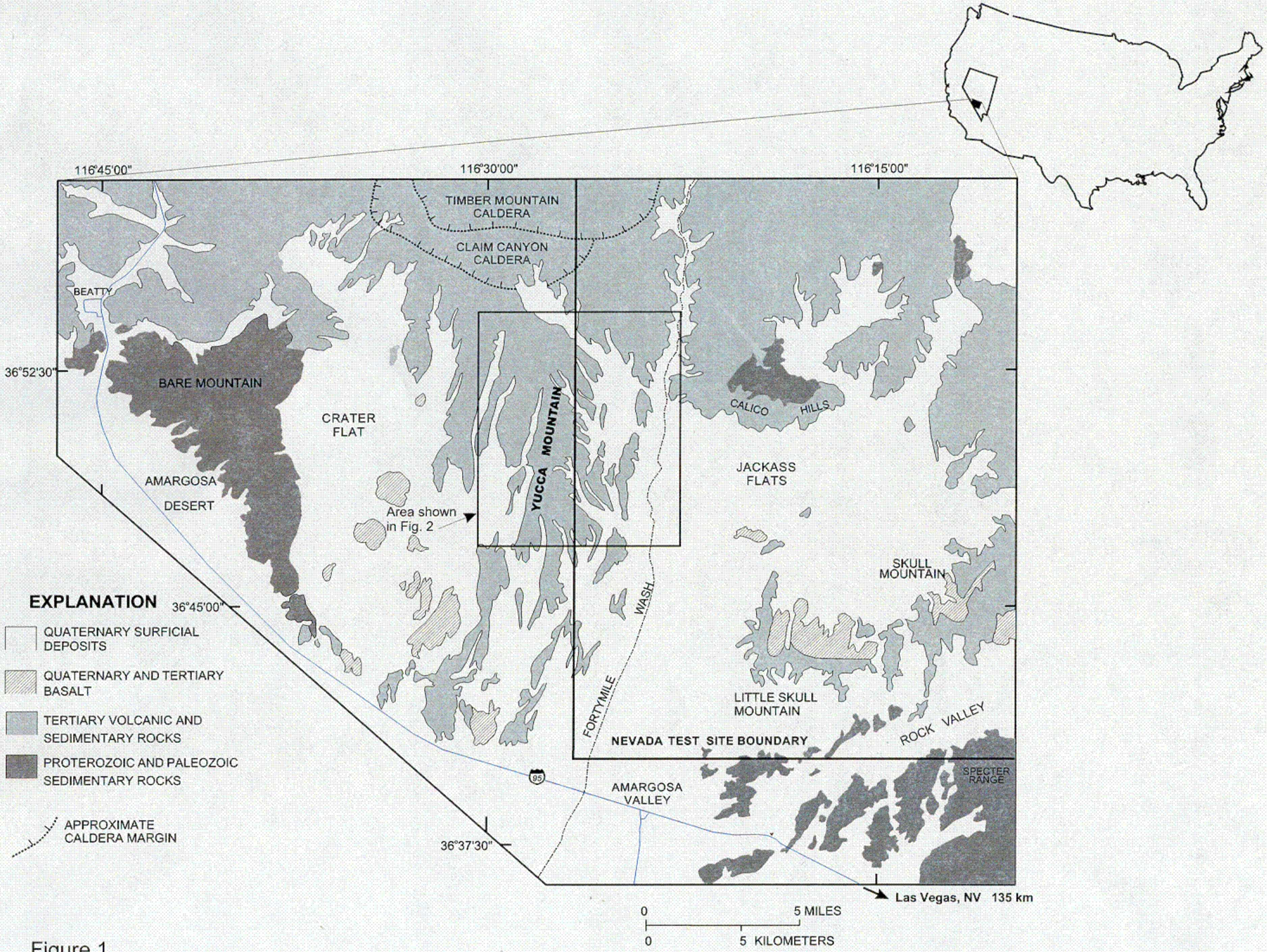

116°45'00"
116°30'00"
116°15'00"
36°52'30"
36°45'00"
36°37'30"
TIMBER MOUNTAIN CALDERA
CLAIM CANYON CALDERA
BEATTY
BARE MOUNTAIN
CRATER FLAT
AMARGOSA DESERT
YUCCA MOUNTAIN
Area shown in Fig. 2
CALICO HILLS
JACKASS FLATS
SKULL MOUNTAIN
LITTLE SKULL MOUNTAIN
FORTYMILE WASH
NEVADA TEST SITE BOUNDARY
ROCK VALLEY
SPECTER RANGE
AMARGOSA VALLEY
95
Las Vegas, NV 135 km
0
5 MILES
0
5 KILOMETERS
EXPLANATION
QUATERNARY SURFICIAL DEPOSITS
QUATERNARY AND TERTIARY BASALT
TERTIARY VOLCANIC AND SEDIMENTARY ROCKS
PROTEROZOIC AND PALEOZOIC SEDIMENTARY ROCKS
APPROXIMATE CALDERA MARGIN

Figure 1

C01


550000
555000
560000
565000
570000
575000
580000
583900
785000
780000
775000
770000
765000
760000
755000
750000
745000
740000
Windy Wash Fault
Fatigue Wash Fault
Solitario Canyon Fault
Bow Ridge Fault
Midway Valley Fault
Paintbrush Canyon Fault
Dune Wash Fault
NRG-6
NR
NP
EH
SDF
DHWF
MD
CD
GDF
IFZ
A6
A7
UZ#16
P#1
AW
SR
SP
EXPLANATION
Quaternary alluvium
Post-Paintbrush Group rocks
Tiva Canyon Tuff
Paintbrush Group bedded tuffs, undivided
Topopah Spring Tuff
Pre-Paintbrush Group rocks
Block-bounding faults
Intrablock faults
Exploratory Studies Facility, Cross-block drift and alcoves
1 0.5 0 1 MILE
1 0.5 0 1 KILOMETER

Figure 2

C02

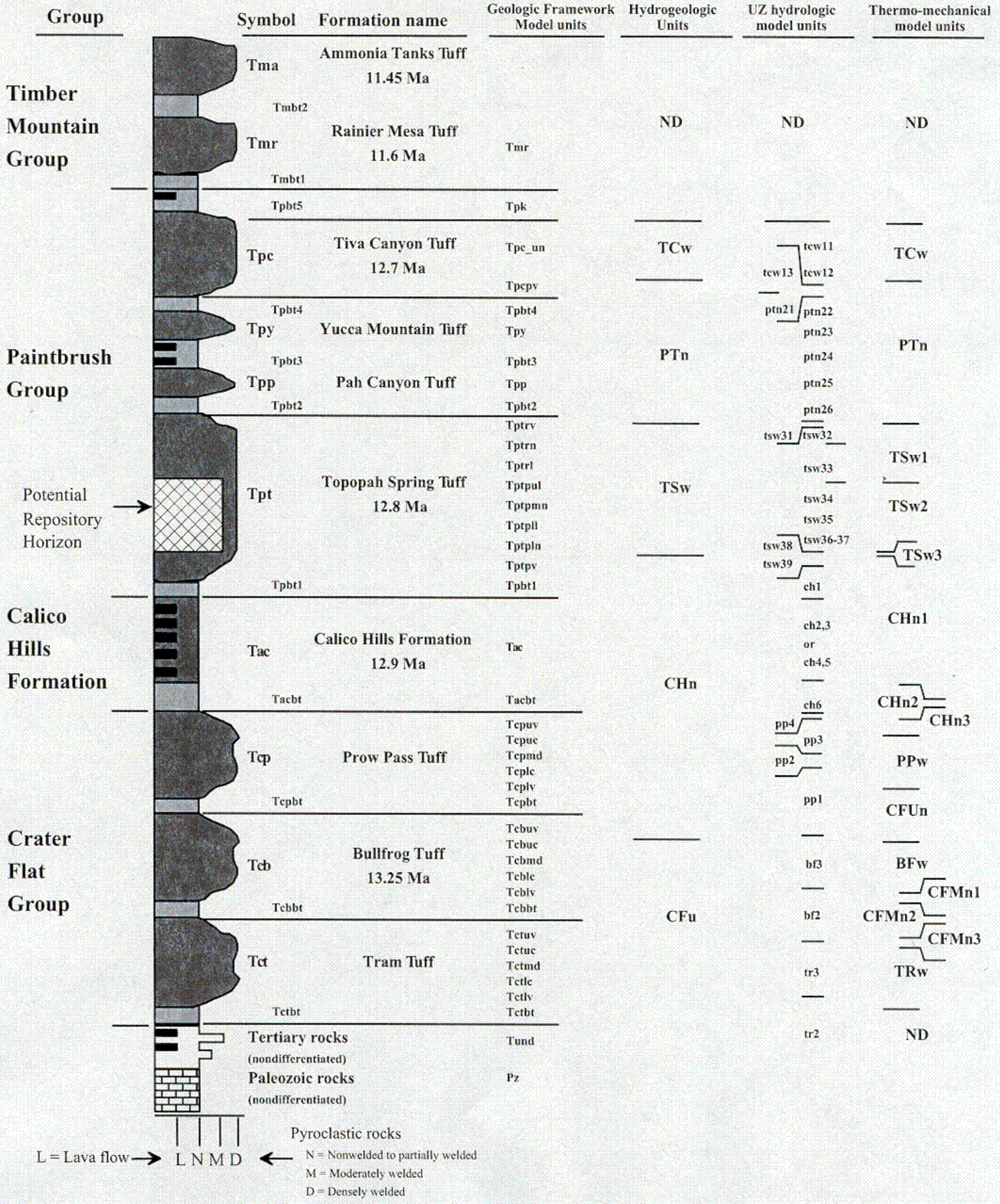
Group
Symbol
Formation name
Geologic Framework Model units
Hydrogeologic Units
UZ hydrologic model units
Thermo-mechanical model units
Timber Mountain Group
Tma
Ammonia Tanks Tuff
11.45 Ma
Tmbt2
Tmr
Rainier Mesa Tuff
11.6 Ma
Tmr
ND
ND
ND
Tmbt1
Tpbt5
Tpk
Tpc
Tiva Canyon Tuff
12.7 Ma
Tpc_un
Tpcpv
TCw
tcw11
tcw13
tcw12
TCw
Paintbrush Group
Tpbt4
Tpbt4
Tpy
Yucca Mountain Tuff
Tpy
ptn21
ptn22
ptn23
Tpbt3
Tpbt3
PTn
ptn24
PTn
Tpp
Pah Canyon Tuff
Tpp
ptn25
Tpbt2
Tpbt2
ptn26
Tptrv
tsw31
tsw32
Tptrn
Tptrl
tsw33
TSw1
Potential Repository Horizon
Tpt
Topopah Spring Tuff
12.8 Ma
Tptpul
Tptpmn
Tptpll
Tptpln
Tptpv
TSw
tsw34
tsw35
TSw2
tsw38
tsw36-37
tsw39
TSw3
Tpbt1
Tpbt1
ch1
Calico Hills Formation
Tac
Calico Hills Formation
12.9 Ma
Tac
CHn
ch2,3
or
ch4,5
CHn1
Tacbt
Tacbt
ch6
CHn2
CHn3
Tcp
Prow Pass Tuff
Tcpuv
Tcpuc
Tcpmd
Tcplc
Tcplv
Tcpbt
pp4
pp3
pp2
pp1
PPw
CFUn
Tcpbt
Crater Flat Group
Tcb
Bullfrog Tuff
13.25 Ma
Tcbuv
Tcbuc
Tcbmd
Tcblc
Tcblv
Tcbbt
bf3
BFw
CFMn1
Tcbbt
CFu
bf2
CFMn2
CFMn3
Tct
Tram Tuff
Tctuv
Tctuc
Tctmd
Tctlc
Tctlv
Tctbt
tr3
TRw
Tctbt
Tertiary rocks
(nondifferentiated)
Tund
tr2
ND
Paleozoic rocks
(nondifferentiated)
Pz
Pyroclastic rocks
L = Lava flow
L N M D
N = Nonwelded to partially welded
M = Moderately welded
D = Densely welded

Figure 3.

C03

UE-25 UZ#16

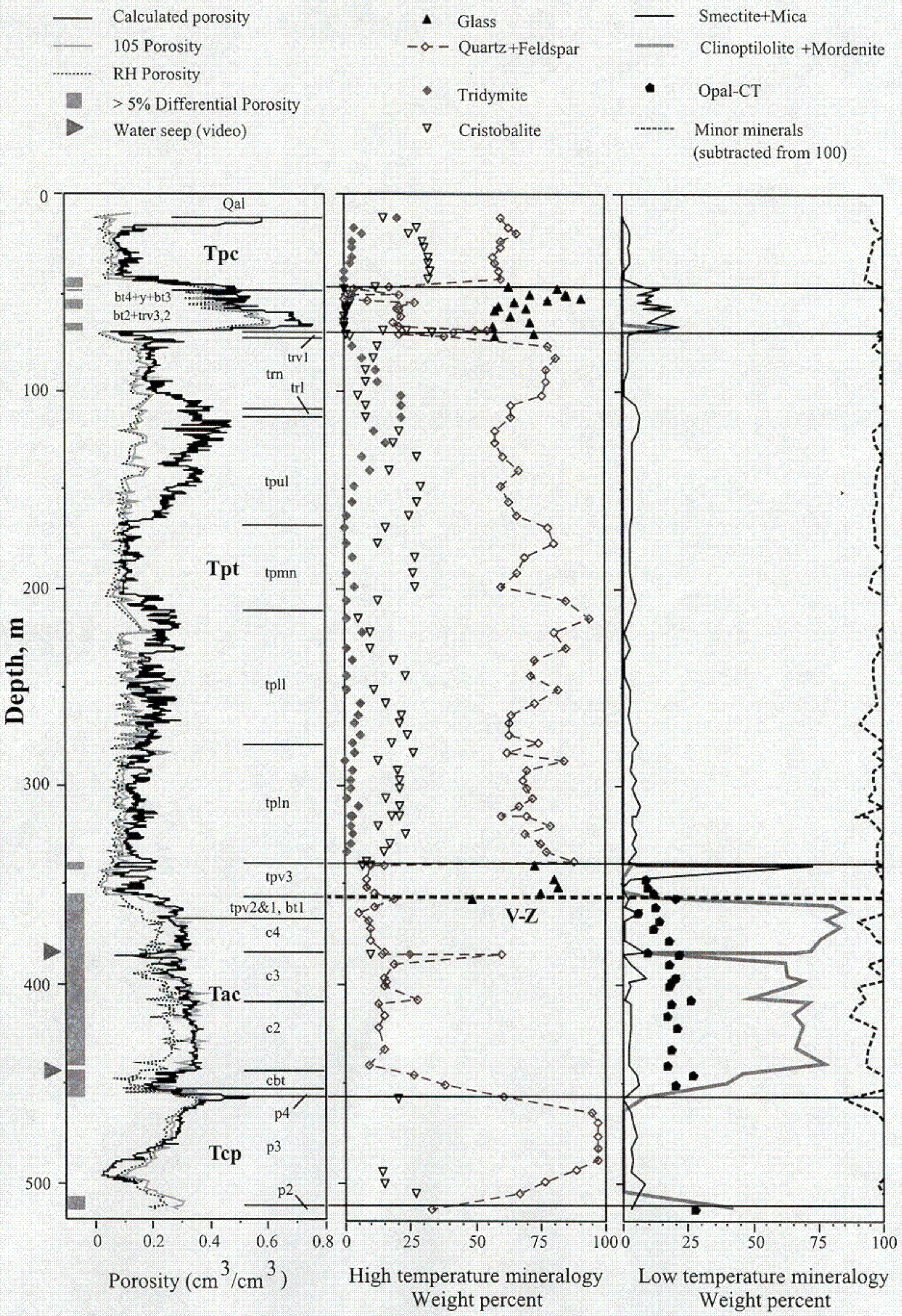

Figure 4.

C04

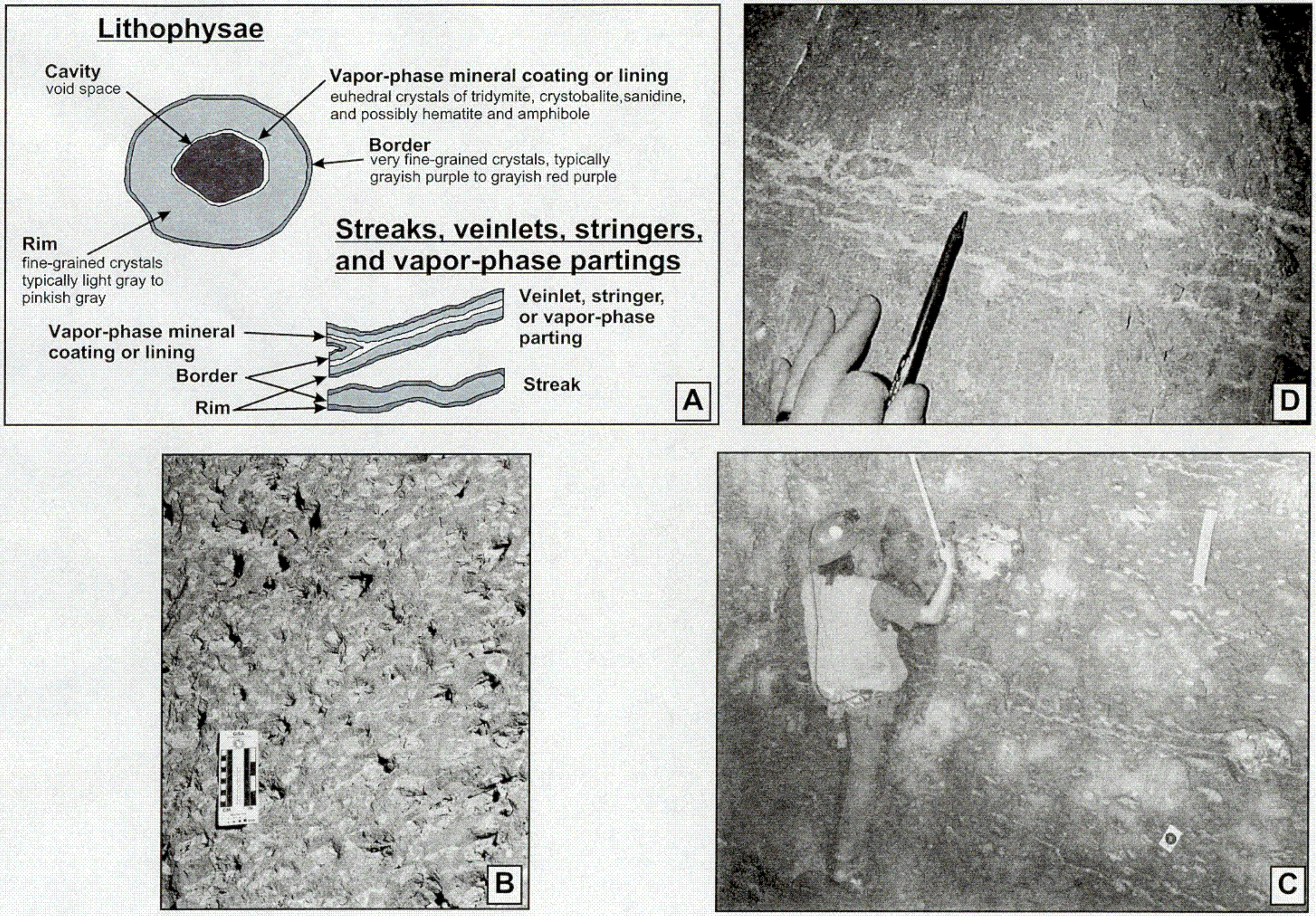
Lithophysae
Cavity
void space
Vapor-phase mineral coating or lining
euhedral crystals of tridymite, crystobalite,sanidine, and possibly hematite and amphibole
Border
very fine-grained crystals, typically grayish purple to grayish red purple
Rim
fine-grained crystals typically light gray to pinkish gray
Streaks, veinlets, stringers, and vapor-phase partings
Vapor-phase mineral coating or lining
Border
Rim
Veinlet, stringer, or vapor-phase parting
Streak
A
D
B
C

Figure 5

C05

NRG-6

Thermal-mechanicalproperties versus depth in the Topopah Spring Tuff and the lower part of the Tiva Canyon Tuff

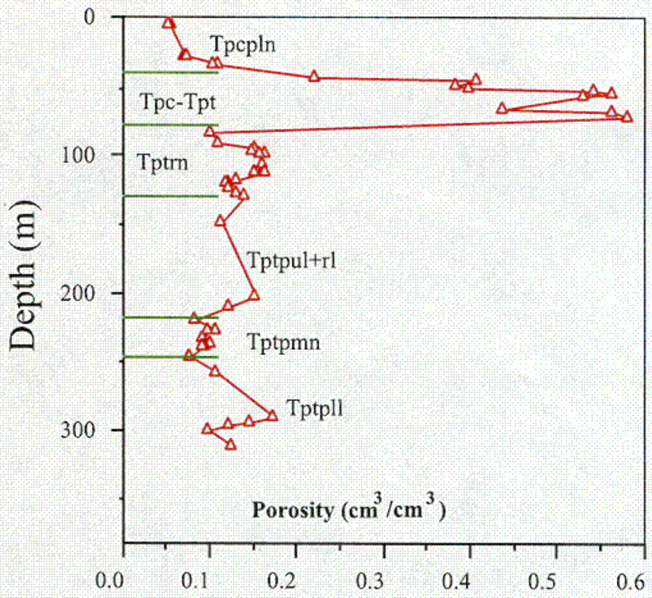

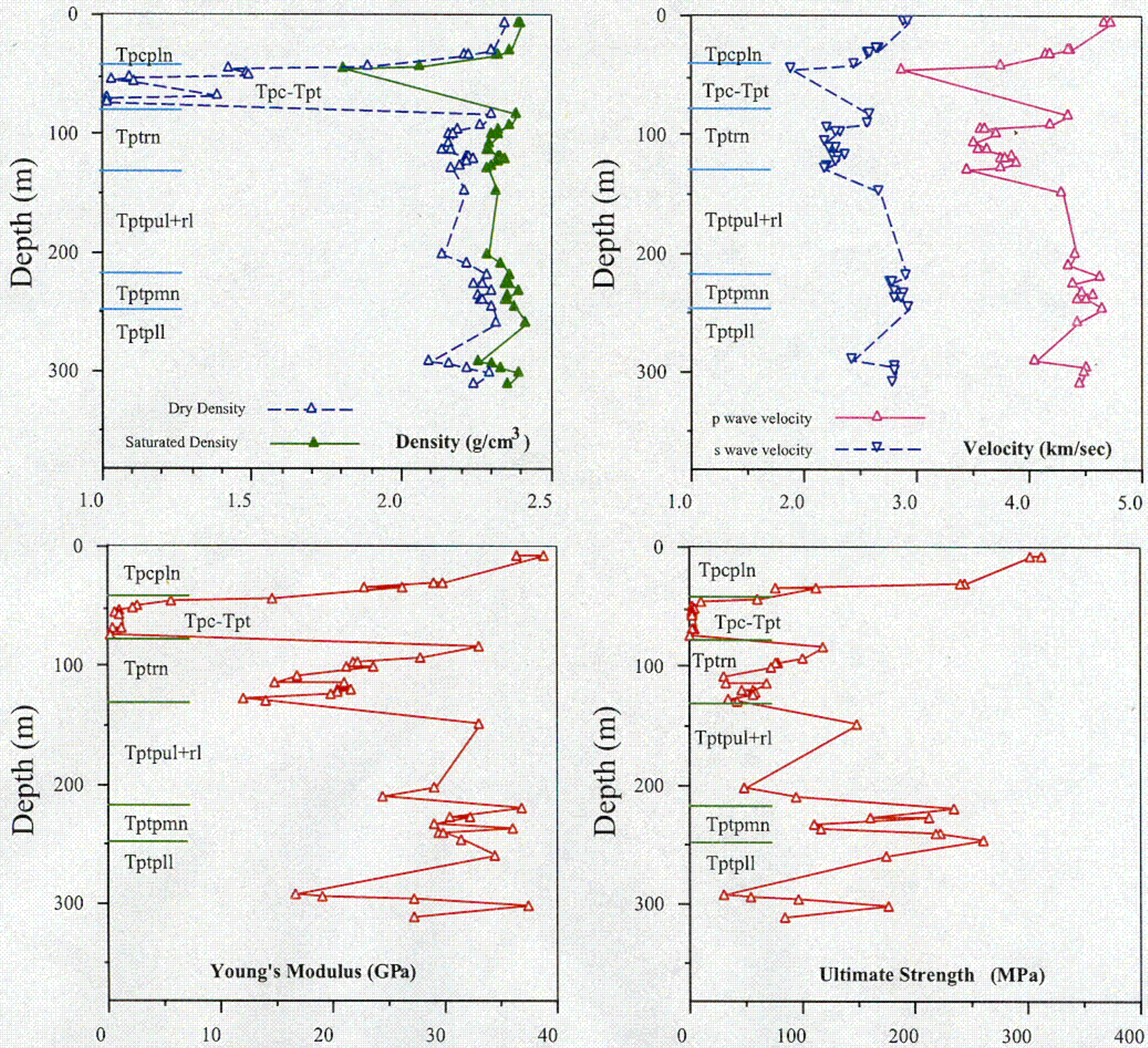

Figure 6.

c06

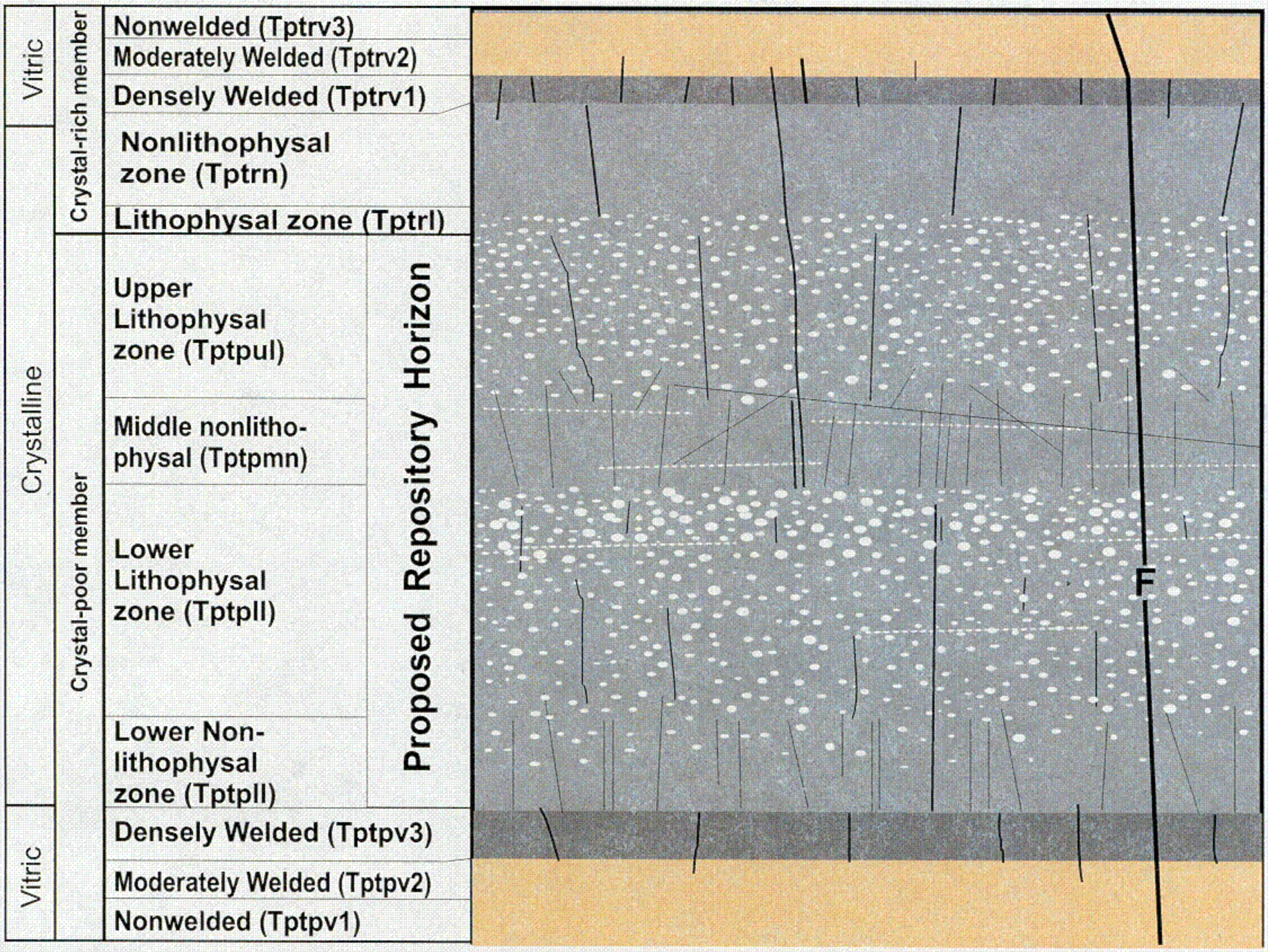

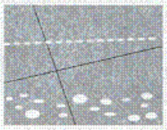

Densely welded, crystalline rocks, white dashed lines indicate vapor-phase partings, white circles and ellipses indicate lithophysae black lines indicate fractures

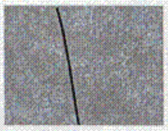

Densely welded, vitric rocks, black lines indicate fractures

Nonwelded to moderately welded, vitric rocks, black lines with "F" designation indicate faults

Figure 7

C07

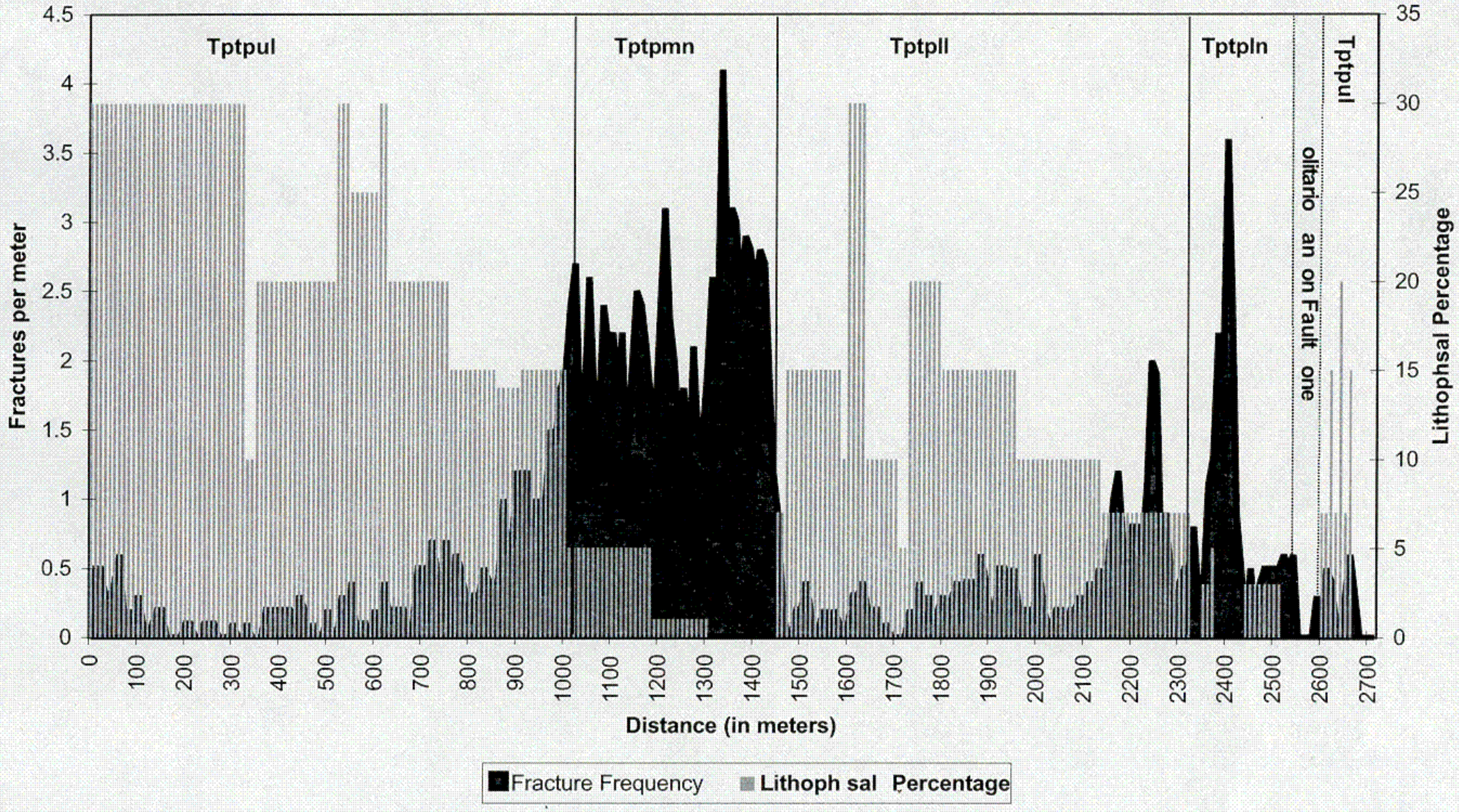
Tptpul
Tptpmn
Tptpll
Tptpln
Tptpul
olitario an on Fault one
Fractures per meter
Lithophsal Percentage
Distance (in meters)
Fracture Frequency
Lithoph sal Percentage
4.5
4
3.5
3
2.5
2
1.5
1
0.5
0
35
30
25
20
15
10
5
0
0
100
200
300
400
500
600
700
800
900
1000
1100
1200
1300
1400
1500
1600
1700
1800
1900
2000
2100
2200
2300
2400
2500
2600
2700

Figure 8

C08

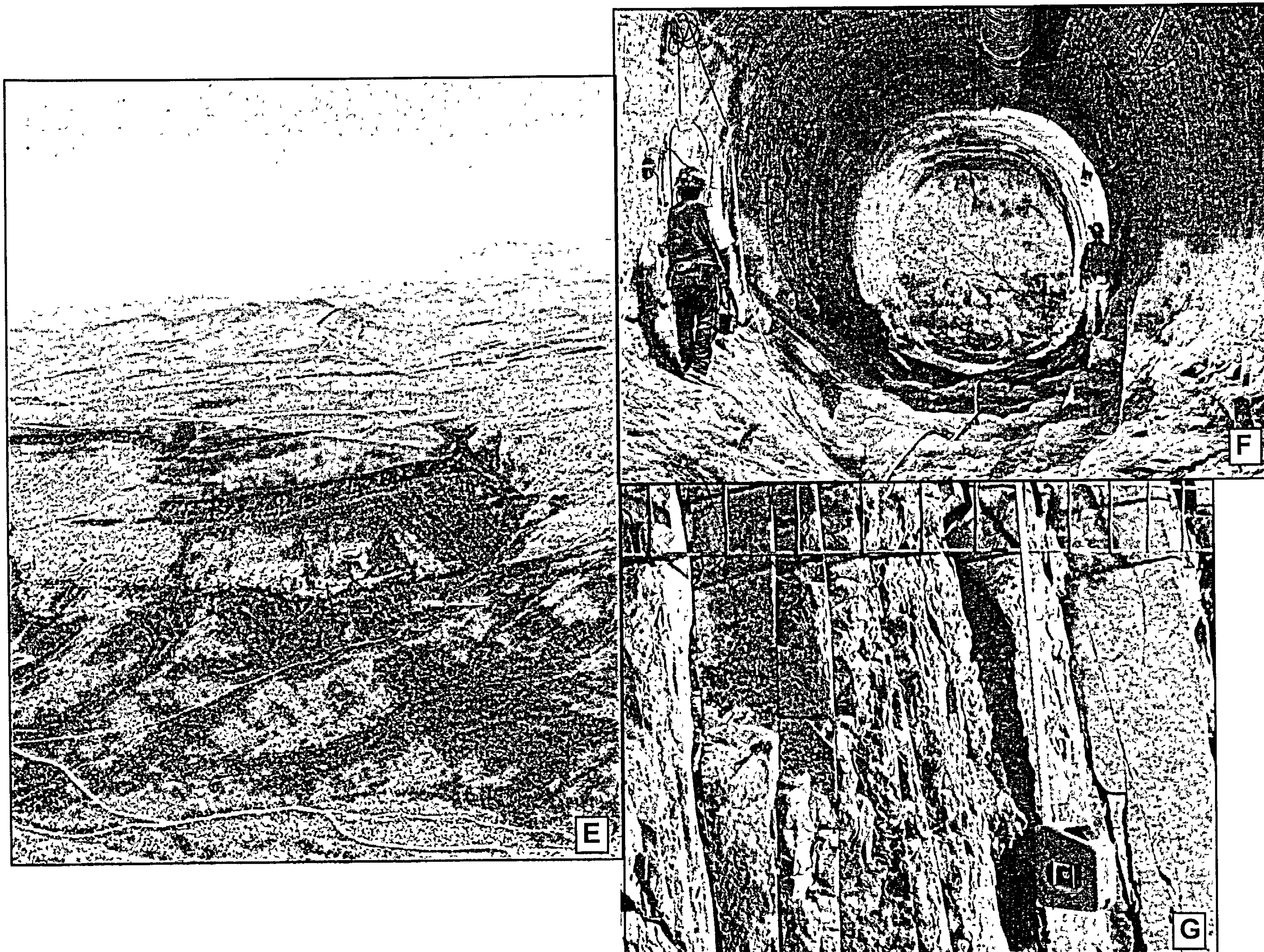

Figure 9